

Supplementary Data

**Unexpected reaction patterns enable simultaneous
differentiation of H₂S, H₂S_n and biothiols**

Wenqiang Chen,^{a*} Li Fu,^a Chunfei Chen,^b Junan Xiao,^a Wenxiu Li,^d Liangliang Zhang,^d Qi Xiao,^a Chusheng Huang,^a Jiarong Sheng,^{a*} and Xiangzhi Song^{c*}

^a Guangxi Key Laboratory of Natural Polymer Chemistry and Physics, Nanning Normal University. Nanning 530001, China.

^b Guangxi Zhuang Autonomous Region Environmental Monitoring Centre, Nanning, 530028, China

^c College of Chemistry & Chemical Engineering, Central South University, Changsha, 410083, China. E-mail: xzsong@csu.edu.cn

^d School of Chemistry and Pharmaceutical Sciences, Guangxi Normal University, Guilin, 541004, China

E-mail: chenwq@csu.edu.cn; shengjiarong99@163.com; xzsong@csu.edu.cn.

Table of Contents

Reagents and Instruments.....	5
Cell Culture and Fluorescence Imaging	5
General procedure for the synthesis of probes.....	6
MCP1	6
MCP2	7
MCP3	7
MCP4	7
MCP5	8
Preparation of compound 7.....	8
Scheme S1.	9
Fig. S1.....	10
Fig. S2.....	11
Fig. S3.....	12
Fig. S4.....	13
Fig. S5.....	13
Fig. S6.....	14
Fig. S7.....	15
Fig. S8.....	16
Fig. S9.....	16
Table S1.....	17
Fig. S10.....	18
Scheme S2.	18
Fig. S11.....	18
Fig. S12.....	19

Fig. S13	19
Fig. S14	19
Fig. S15	20
Fig. S16	21
Fig. S17	22
Fig. S18	22
Fig. S19	22
Fig. S20	23
Fig. S21	23
Fig. S22	24
Fig. S23	24
Fig. S24	25
Fig. S25	25
Fig. S26	26
Fig. S27	26
Fig. S28	27
Fig. S29	28
Fig. S30	29
Fig. S31	30
Fig. S32	31
Fig. S33	32
Fig. S34	33
Fig. S35	34
Fig. S36	34
Fig. S37	35

Fig. S38	35
Fig. S39	36
Fig. S40	36
Fig. S41	37
Fig. S42	37
Fig. S43	38
Fig. S44	38
Fig. S45	39
Fig. S46	39
Fig. S47	40
Fig. S48	40
Fig. S49	41
Fig. S50	41
Fig. S51	42
Fig. S52	42
Fig. S53	43
Fig. S54	43
Fig. S55	44
Fig. S56	44
Fig. S57	45
Fig. S58	45
Fig. S59	46
Fig. S60	46
Fig. S61	47
References	47

Experimental

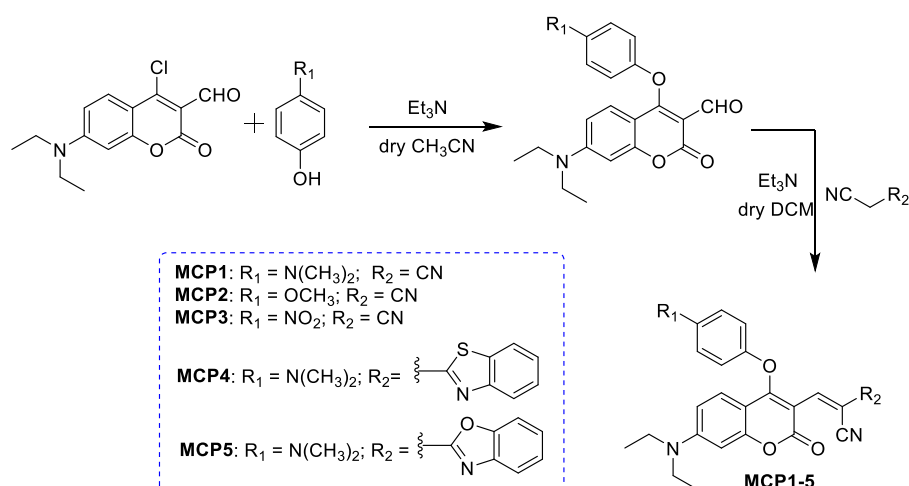
Reagents and Instruments

Dichloromethane, acetonitrile, N,N-dimethylformamide and triethylamine were freshly dehydrated and re-distilled before using. The rest reagents and solvents were purchased from commercial suppliers and used without any further purification. MitoLite™ Deep Red FX660 was purchased from AAT Bioquest ($\lambda_{\text{ex}} = 640 \text{ nm}$, $\lambda_{\text{em}} = 659 \text{ nm}$). LysoBrite™ NIR was purchased from AAT Bioquest ($\lambda_{\text{ex}} = 636 \text{ nm}$, $\lambda_{\text{em}} = 650 \text{ nm}$). ER-Tracker Red was purchased from Beyotime ($\lambda_{\text{ex}} = 587 \text{ nm}$, $\lambda_{\text{em}} = 615 \text{ nm}$). NucView Green Live nucleic acid stain was purchased from GeneCopoeia ($\lambda_{\text{ex}} = 500 \text{ nm}$, $\lambda_{\text{em}} = 530 \text{ nm}$). LPS was purchased from Sigma Aldrich. Deionized water was used throughout all experiments in this work. NMR spectra were recorded on a Bruker 300 MHz, 400 MHz spectrometer using TMS as an internal standard. All accurate mass spectrometric experiments were performed on a Xevo G2 QTof MS (Waters, U.S.A). UV-vis absorption spectra were recorded on an UV-2600 (Shimadzu, Japan) spectrophotometer. Fluorescence spectra were recorded at room temperature using a HITACHI F-4600 fluorescence spectrophotometer with the excitation slit width set at 2.5 nm and the emission slit width at 5.0 nm. TLC analysis was performed on silica gel plates and column chromatography was conducted using silica gel (mesh 200-300), both of which were obtained from Qingdao Ocean Chemicals, China. Infrared (IR) spectra were recorded on a Nicolet iS10 spectrometer (Thermo, U.S.A). The wave numbers (ν) of recorded IR-signals are quoted in cm^{-1} . Fluorescence imaging experiments were recorded on a Zeiss LSM 710 confocal microscope.

Cell Culture and Fluorescence Imaging

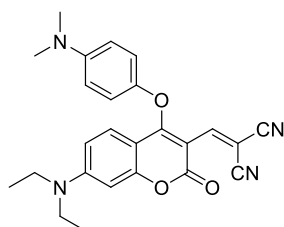
RAW264.7 cells were acquired from the first affiliated hospital of Guangxi Medical University and grown in culture media (DMEM supplemented with 10% fetal bovine serum and 50 unit/mL of penicillin) at 37 °C in a humidified incubator. Prior to the imaging experiments, RAW264.7 cells were seeded in a 12-well plate. The excitation wavelength and band pass for each channel are as follows: blue, $\lambda_{\text{ex}} = 405 \text{ nm}$, $\lambda_{\text{em}} = 420\text{-}470 \text{ nm}$; green, $\lambda_{\text{ex}} = 405 \text{ nm}$, $\lambda_{\text{em}} = 520\text{-}550 \text{ nm}$; red, $\lambda_{\text{ex}} = 488 \text{ nm}$, $\lambda_{\text{em}} = 580\text{-}650 \text{ nm}$.

General procedure for the synthesis of probes

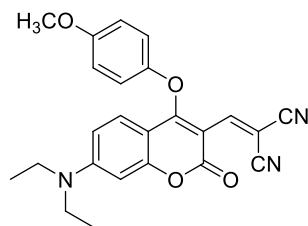


To a stirred solution of 4-chloro-7-diethylamino-coumarin^[1] (27.9 mg, 0.1 mmol, 1.0 equiv) in anhydrous acetonitrile (2 mL) were added the respective phenol (0.1 mmol, 1.0 equiv) and anhydrous NEt₃ (28 μL, 0.2 mmol, 2.0 equiv). The mixture was stirred at 80 °C for 4 hours. After removal of the solvent under a reduced pressure, the obtained residue was re-dissolved by 2 mL anhydrous dichloromethane. To the stirred solution, respective nitriles (0.1 mmol, 1.0 equiv) and anhydrous NEt₃ (42 μL, 0.3 mmol, 3.0 equiv) were added. The reaction mixture was stirred at room temperature for 3 hours. After removal of the solvent under vacuum, the obtained residue was purified by column chromatography to afford the desired products.

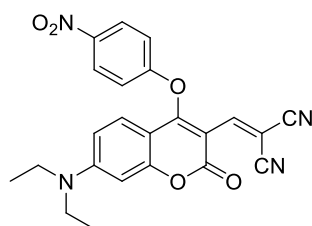
Preparation of MCP1-5



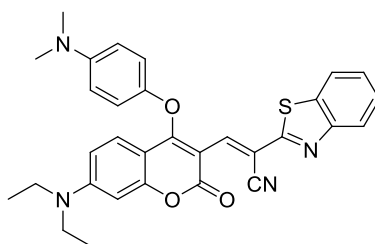
MCP1: General procedure with 4-(dimethylamino)phenol and malononitrile. Yield, 36.4 mg (0.085 mmol, 85%) as a red solid. Mp = 114-117 °C. ¹H NMR (300 MHz, CDCl₃) δ 7.67 (s, 1H), 7.35 (d, *J* = 9.9 Hz, 1H), 6.93 (d, *J* = 9.3 Hz, 2H), 6.71 (d, *J* = 9.0 Hz, 2H), 6.50 (d, *J* = 2.1 Hz, 1H), 6.47 (s, 1H), 3.46 (q, *J* = 7.2 Hz, 4H), 1.32-1.17 (m, 6H). ¹³C NMR (75 MHz, CDCl₃) δ 166.8, 159.9, 157.6, 153.3, 150.2, 127.7, 117.9, 115.2, 113.7, 112.8, 109.9, 103.3, 101.9, 97.1, 83.3, 45.2, 41.0, 12.5. HRMS (ESI) *m/z*: calcd for C₂₅H₂₄N₄NaO₃⁺ [M+Na]⁺ 451.1741 found 451.1741. FTIR(KBr) ν_{max}/cm⁻¹ 3126, 2980, 2218, 1728, 1618, 1546, 1492, 1452, 1418, 1347, 1270, 1201, 1144, 1058, 903, 819, 779.



MCP2: General procedure with 4-methoxyphenol and malononitrile. Yield: 30.7 mg (0.074 mmol, 74%) as a red solid. Mp = 127-130 °C. ¹H NMR (400 MHz, CDCl₃) δ 7.68 (s, 1H), 7.28 (d, J = 8.6 Hz, 1H), 6.96 (d, J = 8.9 Hz, 2H), 6.88 (d, J = 8.9 Hz, 2H), 6.48 (d, J = 8.3 Hz, 2H), 3.81 (s, 3H), 3.45 (q, J = 6.7 Hz, 4H), 1.23 (t, J = 7.1 Hz, 6H). ¹³C NMR (100 MHz, CDCl₃) δ 166.3, 159.8, 157.7, 156.5, 153.5, 150.7, 149.8, 127.7, 117.7, 115.3, 115.2, 112.8, 110.1, 103.2, 102.5, 97.1, 83.3, 55.7, 45.3, 12.5. HRMS (ESI) m/z: calcd for C₂₄H₂₂N₃O₄⁺ [M+H]⁺ 416.1605 found 416.1609. FTIR (KBr) ν_{max}/cm⁻¹ 3107, 3048, 2969, 2927, 2852, 2217, 1725, 1616, 1562, 1498, 1419, 1349, 1247, 1202, 1144, 1081, 939, 895, 815, 776, 747, 602, 533, 461.

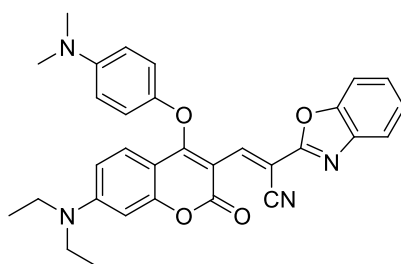


MCP3: General procedure with 4-nitrophenol and malononitrile. Yield: 24.9 mg (0.058 mmol, 58%) as a red solid. Mp = 208-211 °C. ¹H NMR (300 MHz, CDCl₃) δ 8.30 (d, J = 9.3 Hz, 2H), 7.66 (s, 1H), 7.20 (d, J = 9.9 Hz, 1H), 7.16 (d, J = 9.3 Hz, 2H), 6.57-6.54 (m, 2H), 3.50 (q, J = 7.2 Hz, 4H), 1.38-1.07 (m, 6H). ¹³C NMR (75 MHz, CDCl₃) δ 163.7, 160.6, 159.4, 157.7, 154.1, 148.8, 144.1, 127.1, 126.6, 116.4, 114.7, 112.6, 110.8, 110.0, 103.4, 102.8, 97.4, 84.6, 45.5, 12.5. HRMS (ESI) m/z: calcd for C₂₃H₁₈N₄NaO₅⁺ [M+Na]⁺ 453.1169 found 453.1168. FTIR (KBr) ν_{max}/cm⁻¹ 3342, 3116, 2954, 2925, 2855, 2214, 1737, 1622, 1565, 1513, 1497, 1479, 1462, 1425, 1380, 1355, 1339, 1277, 1265, 1219, 1210, 1194, 1170, 1153, 1133, 1110, 1076, 1047, 1006, 885, 855, 830, 809, 777, 751, 713, 679, 613.



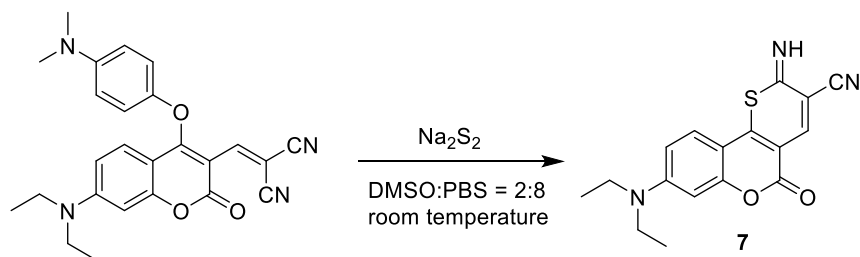
MCP4: General procedure with 4-(dimethylamino)phenol and 2-cyanobenzothiazole. Yield: 6.9 mg (0.013 mmol, 13%) as a yellow solid. Mp = 131-133 °C. ¹H NMR (300

MHz, CDCl₃) δ 8.03 (d, *J* = 7.8 Hz, 1H), 7.90 (s, 1H), 7.84 (d, *J* = 7.2 Hz, 1H), 7.54 (d, *J* = 9.0 Hz, 1H), 7.52-7.44 (m, 1H), 7.43-7.34 (m, 1H), 6.99-6.95 (m, 2H), 6.56 (dd, *J* = 14.7, 9.3 Hz, 4H), 3.46 (q, *J* = 7.2 Hz, 4H), 2.75 (s, 6H), 1.39-1.14 (m, 6H). ¹³C NMR (75 MHz, CDCl₃) δ 164.9, 162.9, 161.4, 156.5, 153.5, 152.3, 148.0, 147.7, 138.9, 134.9, 126.8, 126.6, 125.7, 123.6, 121.4, 118.2, 115.7, 113.7, 110.4, 109.3, 104.4, 102.0, 97.0, 45.0, 40.8, 12.5. HRMS (ESI) *m/z*: calcd for C₃₁H₂₈N₄NaO₃S⁺ [M+Na]⁺ 559.1774 found 559.1740. FTIR(KBr) *v*_{max}/cm⁻¹ 3129, 2954, 2920, 2850, 2227, 1725, 1683, 1617, 1567, 1498, 1455, 1418, 1383, 1353, 1273, 1236, 1203, 1150, 1079, 1013, 886, 813, 766, 716, 669, 595.

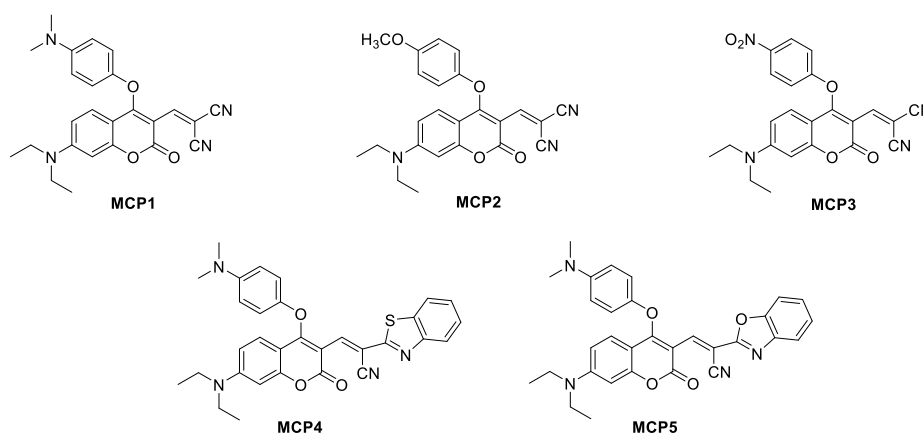


MCP5: General procedure with 4-(dimethylamino)phenol and 2-cyanobenzoxazole. Yield: 12.5 mg (0.024 mmol, 24%) as a yellow solid. Mp = 125-127 °C. ¹H NMR (300 MHz, CDCl₃) δ 8.08 (s, 1H), 7.79-7.68 (m, 1H), 7.55-7.46 (m, 2H), 7.40-7.32 (m, 2H), 6.99 (d, *J* = 9.0 Hz, 2H), 6.68-6.43 (m, 4H), 3.46 (q, *J* = 7.2 Hz, 4H), 1.34-1.10 (m, 6H). ¹³C NMR (75 MHz, CDCl₃) δ 165.1, 161.2, 159.2, 156.8, 152.5, 150.6, 141.8, 140.7, 126.9, 125.8, 124.9, 120.5, 118.1, 114.5, 113.7, 110.5, 109.4, 104.2, 103.5, 102.1, 97.1, 45.1, 40.9, 12.5. HRMS (ESI) *m/z*: calcd for C₃₁H₂₈N₄NaO₄⁺ [M+Na]⁺ 543.2003 found 543.2014. FTIR(KBr) *v*_{max}/cm⁻¹ 3122, 2962, 2925, 2852, 2228, 1725, 1680, 1619, 1567, 1501, 1471, 1451, 1415, 1386, 1353, 1271, 1236, 1200, 1154, 1080, 1018, 886, 810, 768, 716, 669, 599

Preparation of compound 7



To a stirred solution of MCP1 (18.0 mg, 0.04 mmol) in 10 mL PBS buffer (containing 20% DMSO), Na₂S₂ (44 mg, 0.4 mmol) was added. The reaction mixture was stirred at room temperature for 5 min. After completion of the reaction, the mixture was diluted with 200 mL ethyl acetate, the organic layer was then separated and washed with brine (100 mL × 5 times) and dried over MgSO₄. After removal of the solvent under reduced pressure, the resultant residue was further purified by silica gel chromatography to give compound 7 as a red powder (12.3 mg, 90%). Mp = 142-145 °C. ¹H NMR (300 MHz, CDCl₃) δ 8.03 (s, 1H), 7.40 (d, J = 9.3 Hz, 1H), 6.67 (dd, J = 9.3, 2.4 Hz, 1H), 6.44 (d, J = 2.4 Hz, 1H), 3.49 (q, J = 7.2 Hz, 4H), 1.27 (t, J = 7.2 Hz, 6H). ¹³C NMR (75 MHz, d₆-DMSO) δ 158.12, 157.62, 155.20, 154.96, 153.86, 153.31, 143.80, 126.16, 116.26, 111.20, 105.41, 104.85, 97.14, 45.00, 12.83. HRMS (ESI) m/z: calcd for C₁₇H₁₅N₃NaO₂S⁺ [M+Na]⁺ 348.0777 found 348.0775. FTIR (KBr) ν_{max}/cm⁻¹ 3395, 3232, 2960, 2923, 2852, 2219, 1724, 1611, 1500, 1419, 1351, 1261, 1136, 1078, 1017, 799, 756, 660, 494.



Scheme S1. Chemical structures of MCP 1-5.

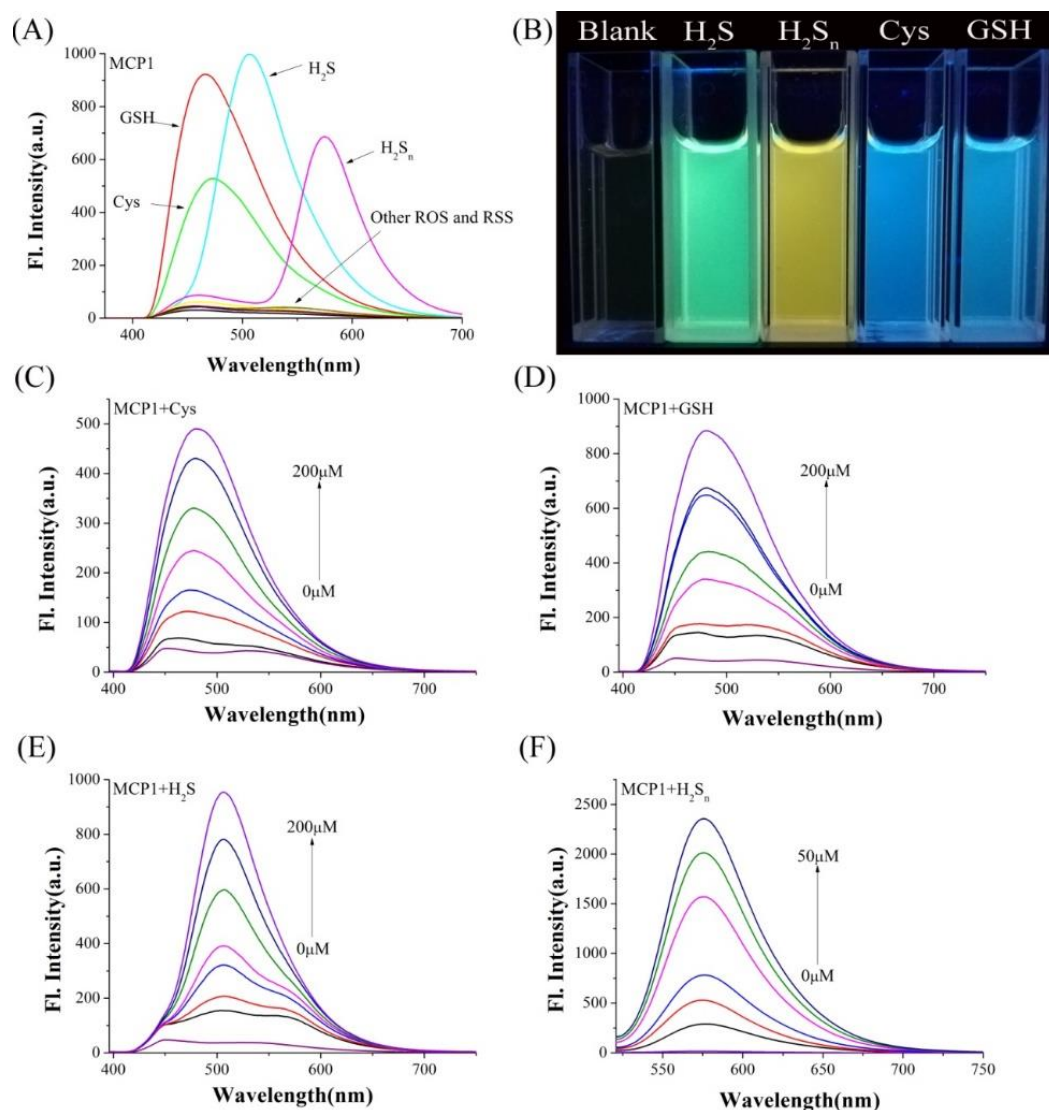


Fig. S1 (A) Fluorescence spectra of **MCP1** (10 μM) in the presence of various agents (200 μM for each): H_2S , H_2S_n , $\text{S}_2\text{O}_3^{2-}$, SO_3^{2-} , SO_4^{2-} , HSO_3^- , Cys, GSH, H_2O_2 , ClO^- , O_2^- (excited at 365 nm, excitation and emission slits: 2.5/5.0 nm). (B) Fluorescence photos of **MCP1** (10 μM) in the absence and presence of 50.0 equiv of Cys, GSH, H_2S , and H_2S_n in PBS buffer (10 mM, pH 7.4, mixed with 20% DMSO) at 25 $^\circ\text{C}$ under illumination by a 365 nm UV lamp. (C-E) Fluorescence spectra of **MCP1** (10 μM) after the addition of incremental dose (0-200 μM) of Cys (C), GSH (D), H_2S (E) in PBS buffer (10 mM, pH 7.4, mixed with 20% DMSO) (excited at 386 nm, excitation and emission slits: 2.5/5.0 nm). (F) Fluorescence spectra of **MCP1** (10 μM) after the addition of incremental dose (0-50 μM) of H_2S_n (excited at 511 nm, excitation and emission slits: 2.5/5.0 nm).

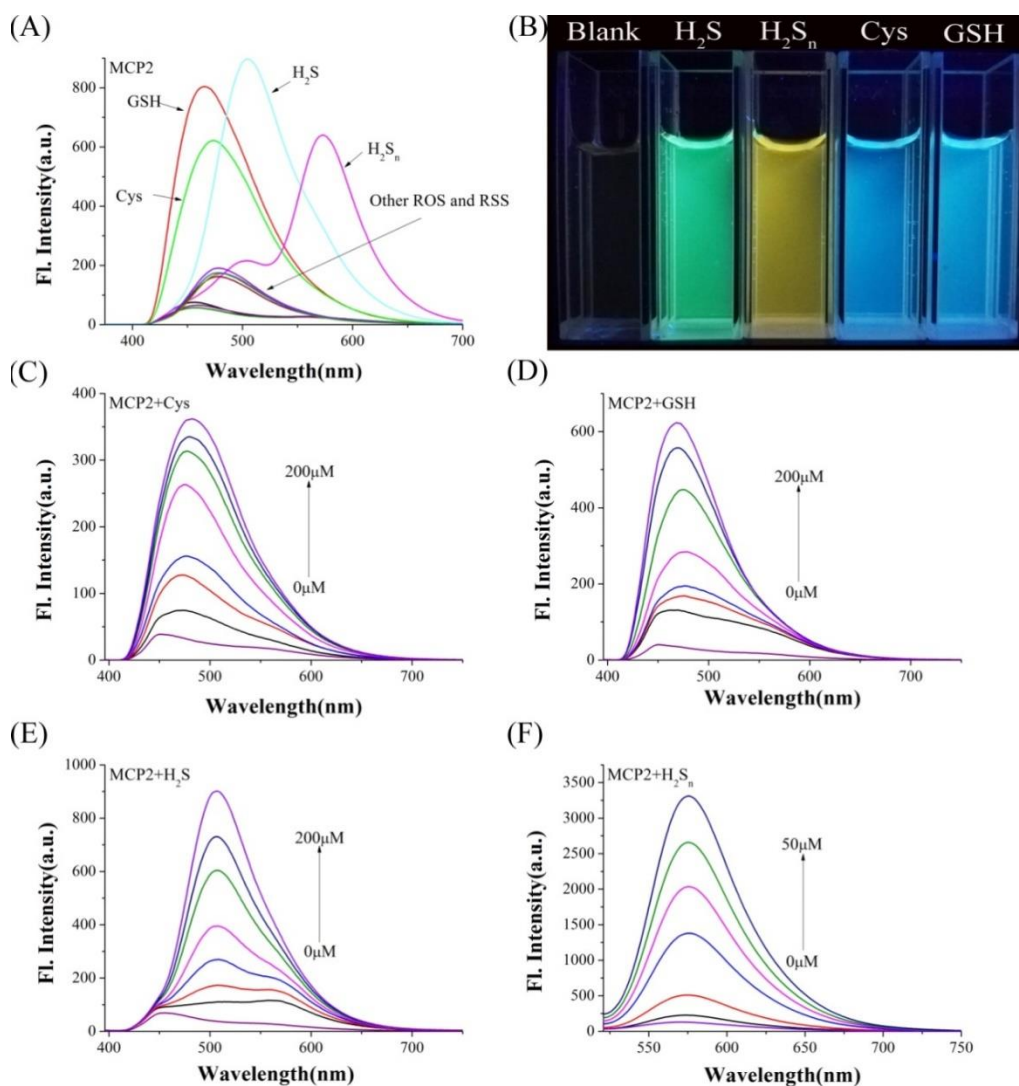


Fig. S2 (A) Fluorescence spectra of **MCP2** (10 μM) in the presence of various agents (200 μM for each): H_2S , H_2S_n , $\text{S}_2\text{O}_3^{2-}$, SO_3^{2-} , SO_4^{2-} , HSO_3^- , Cys, GSH, H_2O_2 , ClO^- , O_2^- (excited at 365 nm, Slits: 2.5/5.0 nm). (B) Fluorescence photos of **MCP2** (10 μM) in the absence and presence of 50.0 equiv of Cys, GSH, H_2S , and H_2S_n in PBS buffer (10 mM, pH 7.4, mixed with 20% DMSO) at 25 $^\circ\text{C}$ under illumination by a 365nm UV lamp. (C-E) Fluorescence spectra of **MCP2** (10 μM) after the addition of incremental dose (0-200 μM) of Cys (C), GSH (D), H_2S (E) in PBS buffer (10 mM, pH 7.4, mixed with 20% DMSO) (excited at 386 nm, excitation and emission slits: 2.5/5.0 nm). (F) Fluorescence spectra of **MCP2** (10 μM) after the addition of incremental dose (0-50 μM) of H_2S_n (excited at 511 nm, excitation and emission slits: 2.5/5.0 nm).

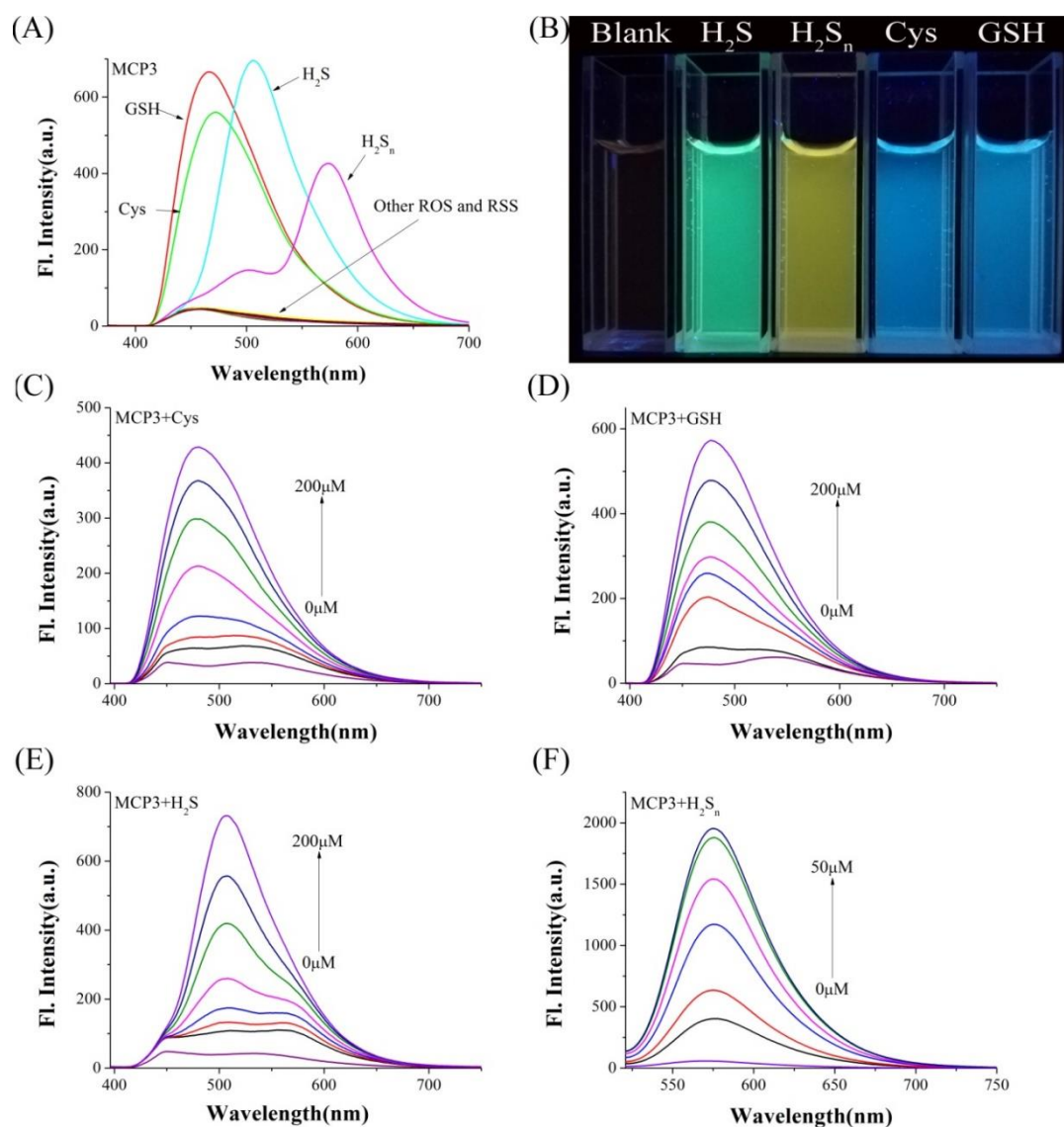


Fig. S3 (A) Fluorescence spectra of **MCP3** (10 μM) in the presence of various agents (200 μM for each): H₂S, H₂S_n, S₂O₃²⁻, SO₃²⁻, SO₄²⁻, HSO₃⁻, Cys, GSH, H₂O₂, ClO⁻, O₂⁻ (excited at 365 nm, excitation and emission slits: 2.5/5.0 nm). (B) Fluorescence photos of **MCP3** (10 μM) in the absence and presence of 50.0 equiv of Cys, GSH, H₂S, and H₂S_n in PBS buffer (10 mM, pH 7.4, mixed with 20% DMSO) at 25 °C under illumination by a 365nm UV lamp. (C-E) Fluorescence spectra of **MCP3** (10 μM) after addition of incremental dose (0-200 μM) of Cys (C), GSH (D), H₂S (E) in PBS buffer (10 mM, pH 7.4, mixed with 20% DMSO) (excited at 386 nm, excitation and emission slits: 2.5/5.0 nm). (F) Fluorescence spectra of **MCP3** (10 μM) after addition of incremental dose (0-50 μM) of H₂S_n (excited at 511 nm, excitation and emission slits: 2.5/5.0 nm)

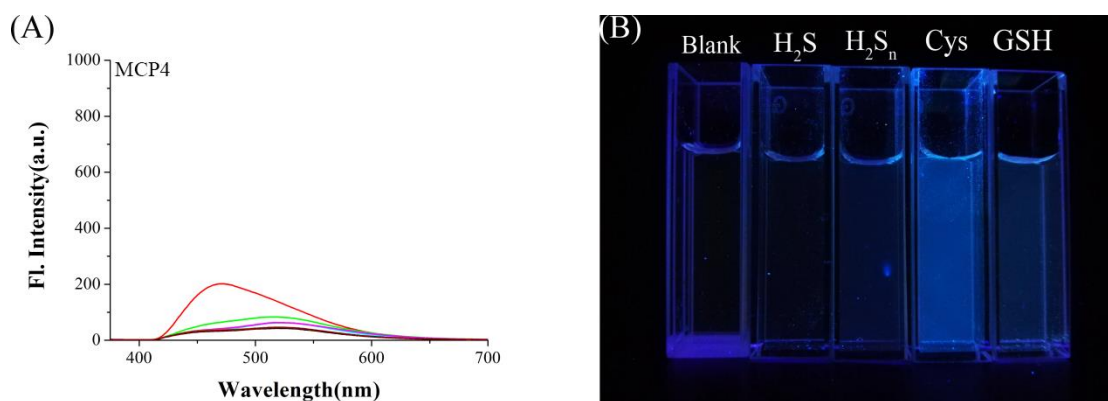


Fig. S4 (A) Fluorescence spectra of **MCP4** (10 μM) in the presence of various agents (200 μM for each): H_2S , H_2S_n , $\text{S}_2\text{O}_3^{2-}$, SO_3^{2-} , SO_4^{2-} , HSO_3^- , Cys, GSH, H_2O_2 , ClO^- , O_2^- (excited at 365 nm, excitation and emission slits: 2.5/5.0 nm). (B) Fluorescence photos of **MCP4** (10 μM) in the absence and presence of 50.0 equiv of Cys, GSH, H_2S , and H_2S_n in PBS buffer (10 mM, pH 7.4, mixed with 20% DMSO) at 25 $^\circ\text{C}$ under illumination by a 365nm UV lamp.

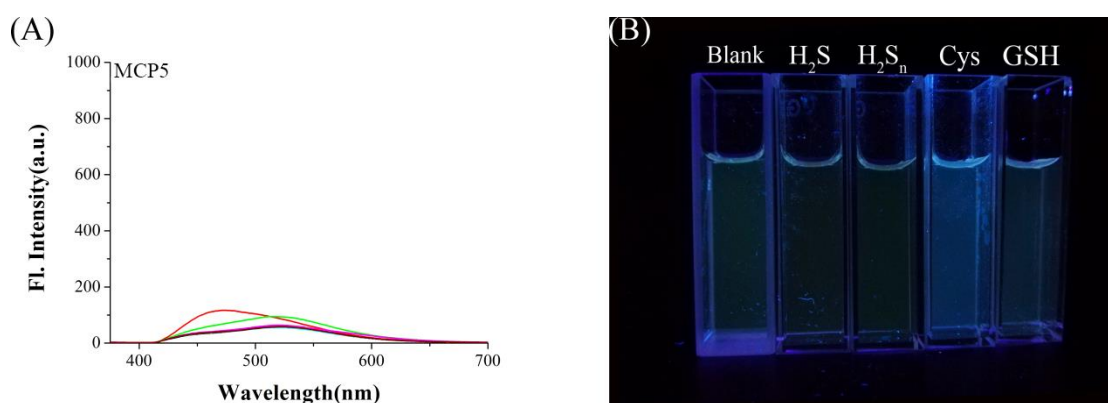


Fig. S5 (A) Fluorescence spectra of **MCP5** (10 μM) in the presence of various agents (200 μM for each): H_2S , H_2S_n , $\text{S}_2\text{O}_3^{2-}$, SO_3^{2-} , SO_4^{2-} , HSO_3^- , Cys, GSH, H_2O_2 , ClO^- , O_2^- (excited at 365 nm, excitation and emission slits: 2.5/5.0 nm). (B) Fluorescence photos of **MCP5** (10 μM) in the absence and presence of 50.0 equiv of Cys, GSH, H_2S , and H_2S_n in PBS buffer (10 mM, pH 7.4, mixed with 20% DMSO) at 25 $^\circ\text{C}$ under illumination by a 365nm UV lamp.

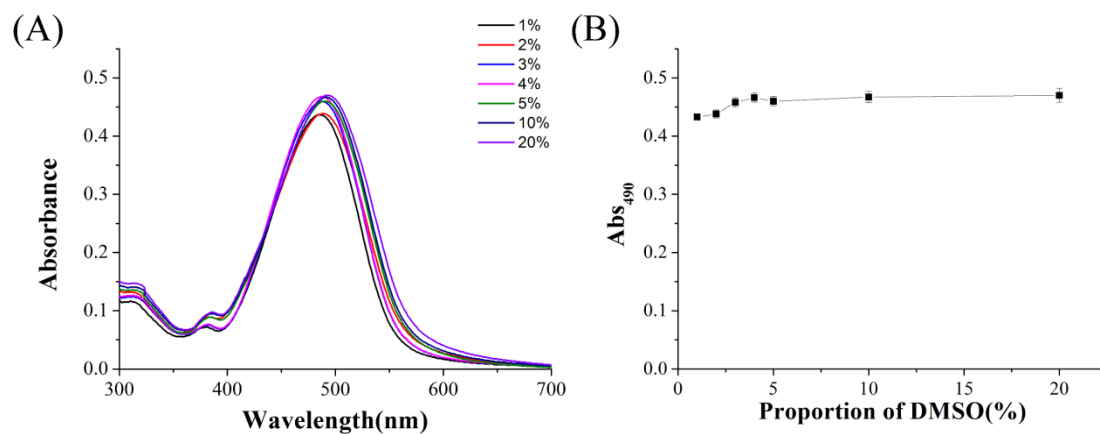


Fig. S6 (A) Uv-vis spectra of **MCP1** (10 μ M) in PBS buffer (10 mM, pH 7.4, mixed with different contents of DMSO) at 25 $^{\circ}$ C. (B) The related Uv-vis absorbance changes of **MCP1** at 490 nm versus different contents of DMSO.

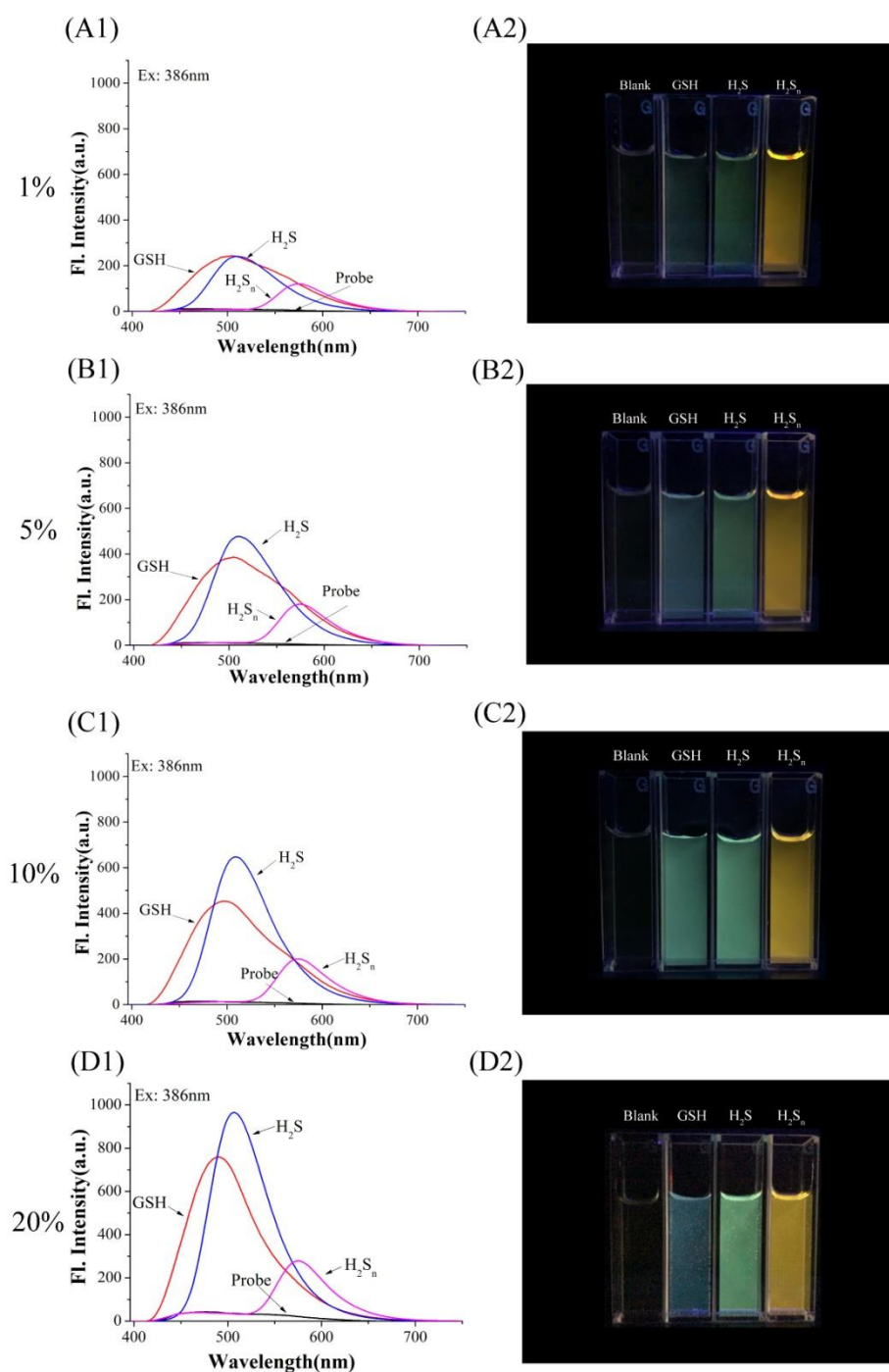


Fig. S7 (A1-D1) Fluorescence spectra of **MCP1** (10 μM) in the presence of various agents (200 μM for each): GSH, H₂S, H₂S_n (excited at 386 nm, excitation and emission slits: 2.5/5.0 nm) in PBS buffer (10 mM, pH 7.4, mixed with 1-20% DMSO) at 25 $^{\circ}\text{C}$. (A2-D2) Fluorescence photos of **MCP1** (10 μM) in the absence and presence of 200 μM of GSH, H₂S, H₂S_n in PBS buffer (10 mM, pH 7.4, mixed with 1-20% DMSO) at 25 $^{\circ}\text{C}$ under illumination by a 365 nm UV lamp.

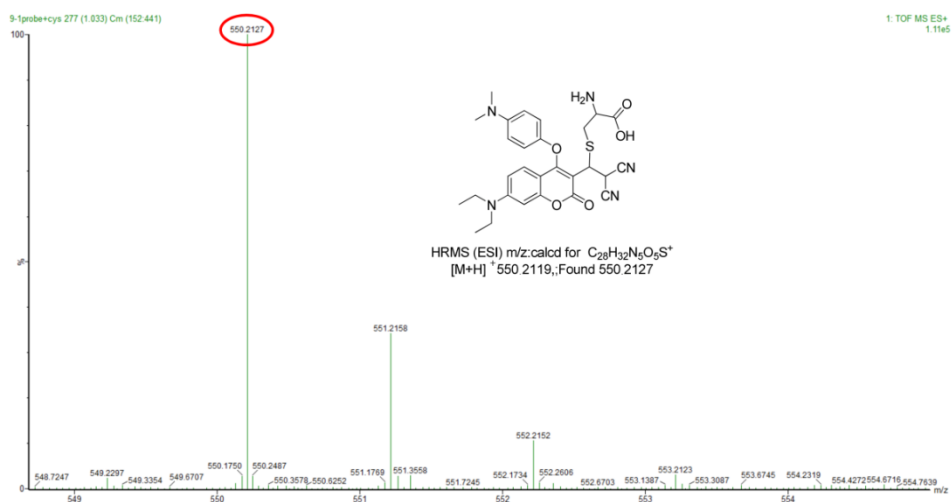


Fig. S8 HRMS of MCP-SCys.

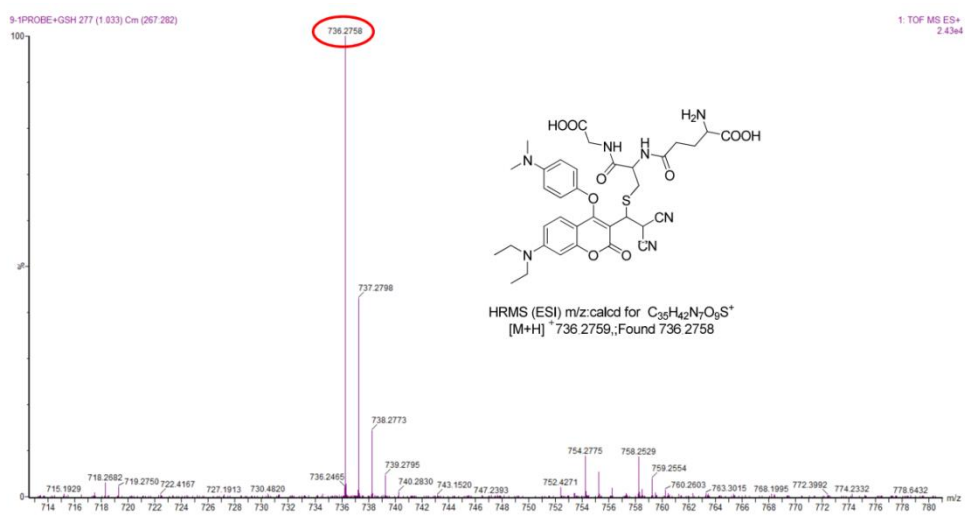
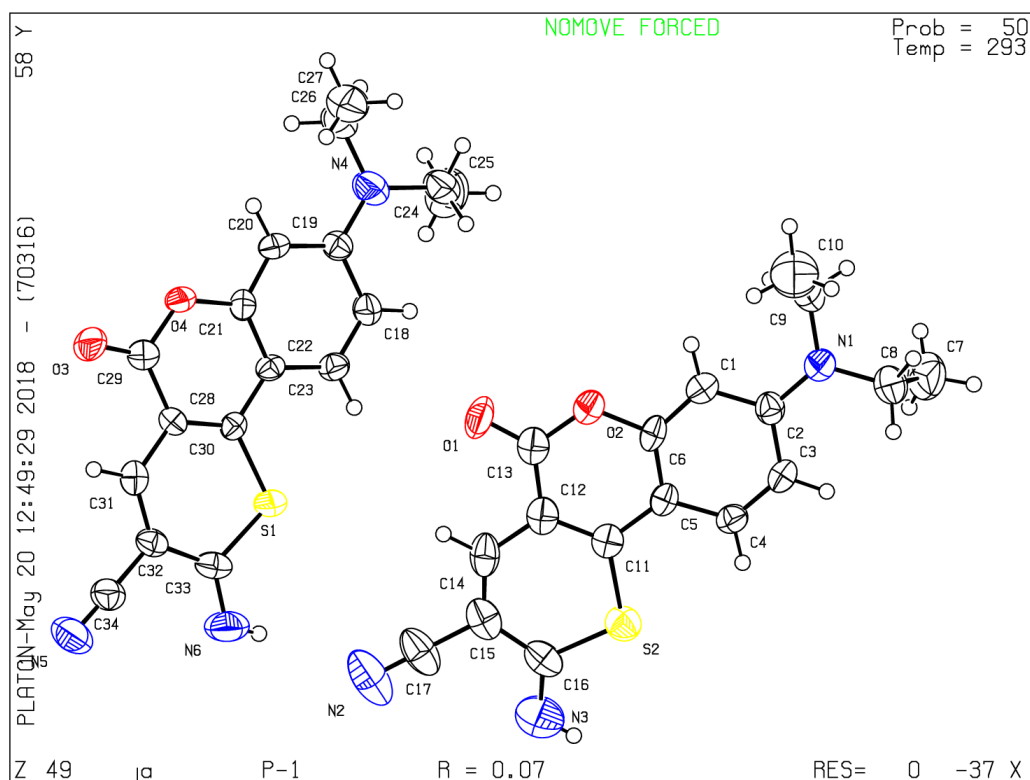


Fig. S9 HRMS of MCP-SGSH.

Table S1. X-ray structures of 7 (with 20% probability level)



Compound :7		CCDC: 1886754	
Bond precision: C-C = 0.0064 Å		Wavelength = 0.71076	
a = 7.6379(8)	b = 13.8560(15)	c = 15.3484(16)	
alpha = 84.804(4)	beta = 85.101(4)	gamma = 74.968(3)	
Cell setting: Triclinic		Moiety formula: C ₁₇ H ₁₅ N ₃ O ₂ S	
Cell volume = 1559.1(3)		Space group: P -1	
Data completeness = 0.997		Theta(max) = 25.680	
R(reflections) = 0.0724(2628)		WR2(reflections) = 0.1657(5911)	
S = 1.006		Radiation type: MoK α	
Measurement device type: CCD area detector		Measurement method: phi and omega scans	
Structure solution: SHELXS-97		Structure refinement: SHELXL-97	
Solution primary: direct		Solution secondary: difmap	
Solution hydrogens: geom		Hydrogen treatment: mixed	

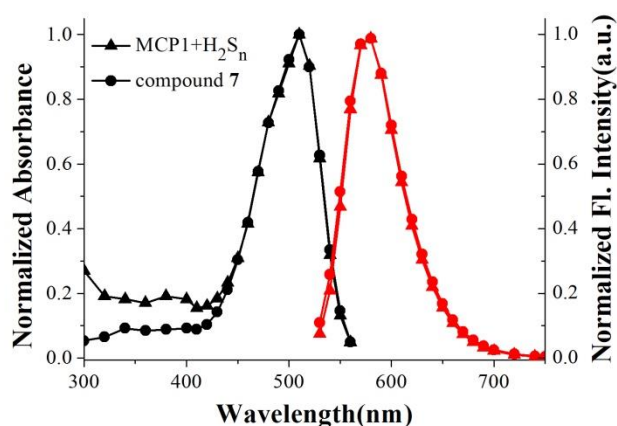
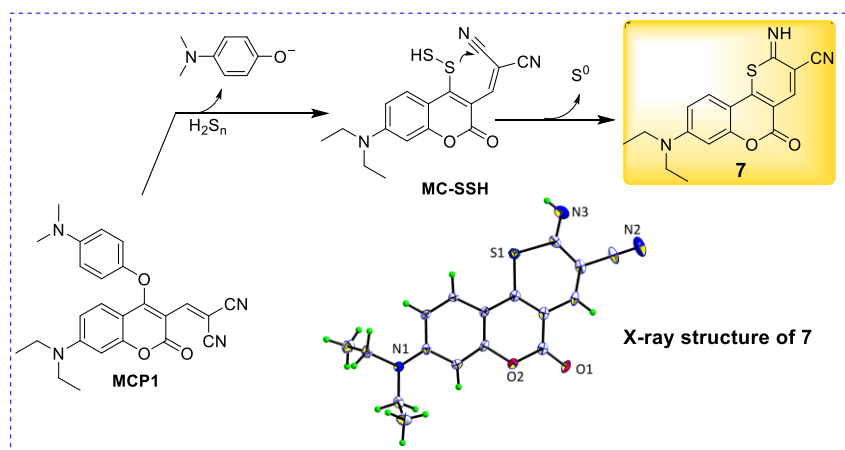


Fig. S10 Normalized UV-vis absorption and fluorescence spectra of MCP1+100.0 equiv Na_2S_2 and compound **7** in PBS buffer (10 mM, pH 7.4, mixed with 20% DMSO) at 25 °C.



Scheme S2. Crystal structure of **7** and the proposed mechanism of **7** formation.

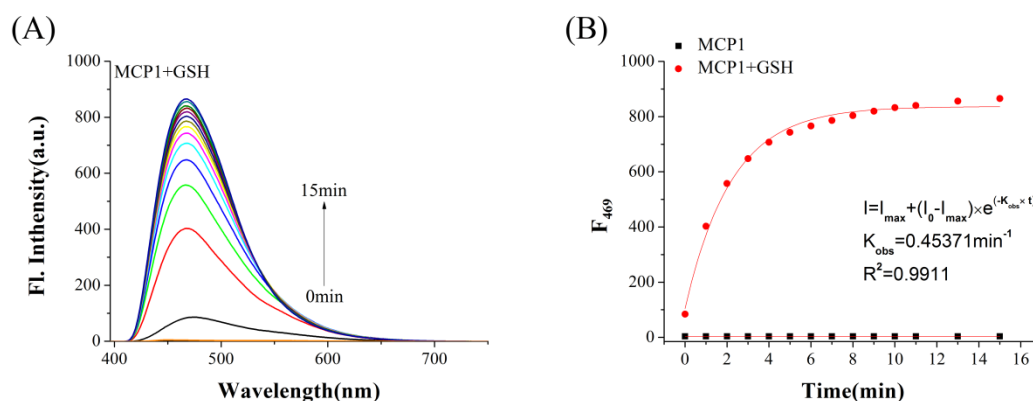


Fig. S11 Time-dependent fluorescence behavior of **MCP1** (10 μM) toward 100.0 equiv of **GSH** (excited at 386 nm, excitation and emission slits: 2.5/5.0 nm) in PBS buffer (10 mM, pH 7.4) at 25 °C. (A): fluorescence spectra; (B): plot of fluorescence intensity as a function of time.

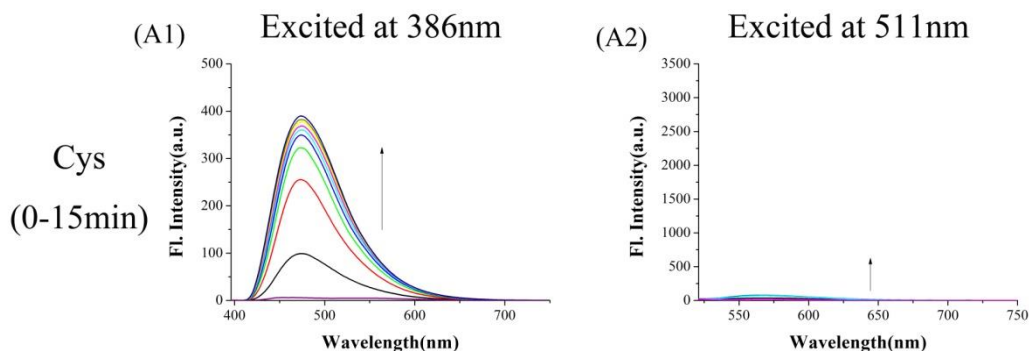


Fig. S12 Time-dependent fluorescence spectra of MCP1 (10 μM) in the presence of 100.0 equiv. of Cys in PBS buffer (10 mM, pH 7.4, mixed with 20% DMSO) at 25 $^{\circ}\text{C}$. (A1) excited at 386 nm; (A2) excited at 511 nm.

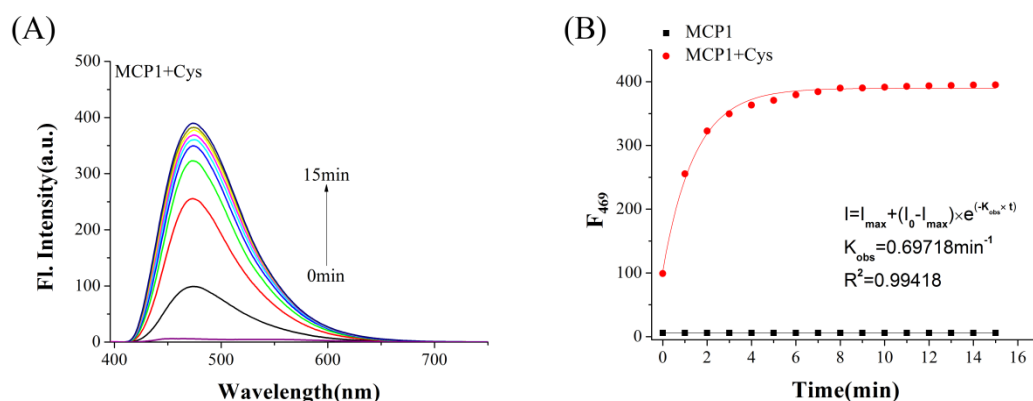


Fig. S13 Time-dependent fluorescence behavior of MCP1 (10 μM) toward 100.0 equiv of Cys (excited at 386 nm, excitation and emission slits: 2.5/5.0 nm) in PBS buffer (10 mM, pH 7.4) at 25 $^{\circ}\text{C}$. (A): fluorescence spectra; (B): plot of fluorescence intensity as a function of time.

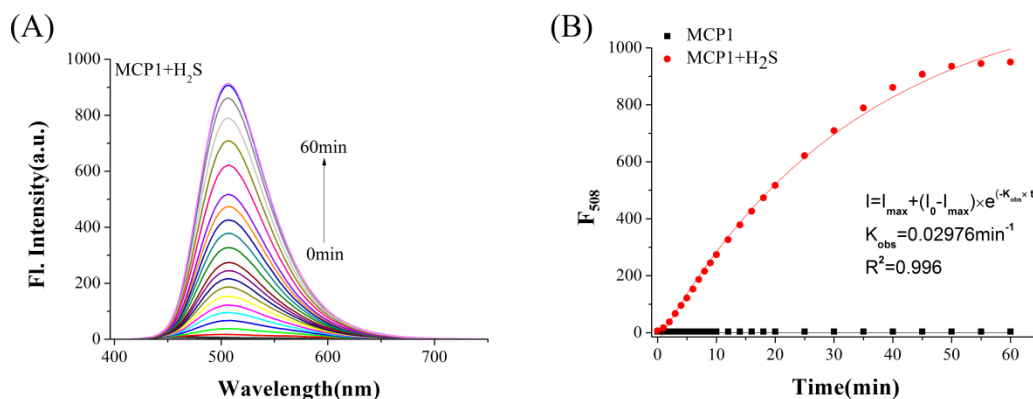


Fig. S14 Time-dependent fluorescence behavior of MCP1 (10 μM) toward 100.0 equiv of H_2S (excited at 386 nm, excitation and emission slits: 2.5/5.0 nm) in PBS buffer (10 mM, pH 7.4) at 25 $^{\circ}\text{C}$. (A): fluorescence spectra; (B): plot of fluorescence intensity as a function of time.

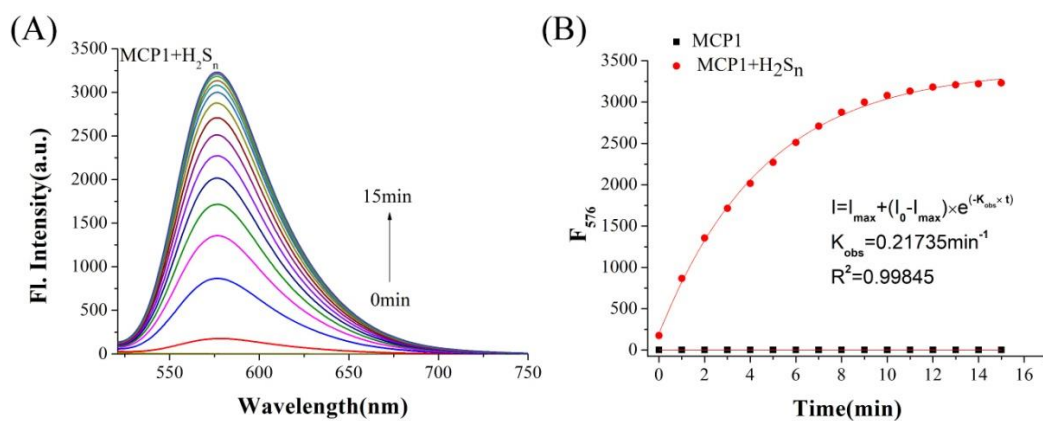


Fig. S15 Time-dependent fluorescence behavior of **MCP1** (10 μM) toward 100.0 equiv of H_2S_n (excited at 386 nm, excitation and emission slits: 2.5/5.0 nm) in PBS buffer (10 mM, pH 7.4) at 25 $^\circ\text{C}$. (A): fluorescence spectra; (B): plot of fluorescence intensity as a function of time.

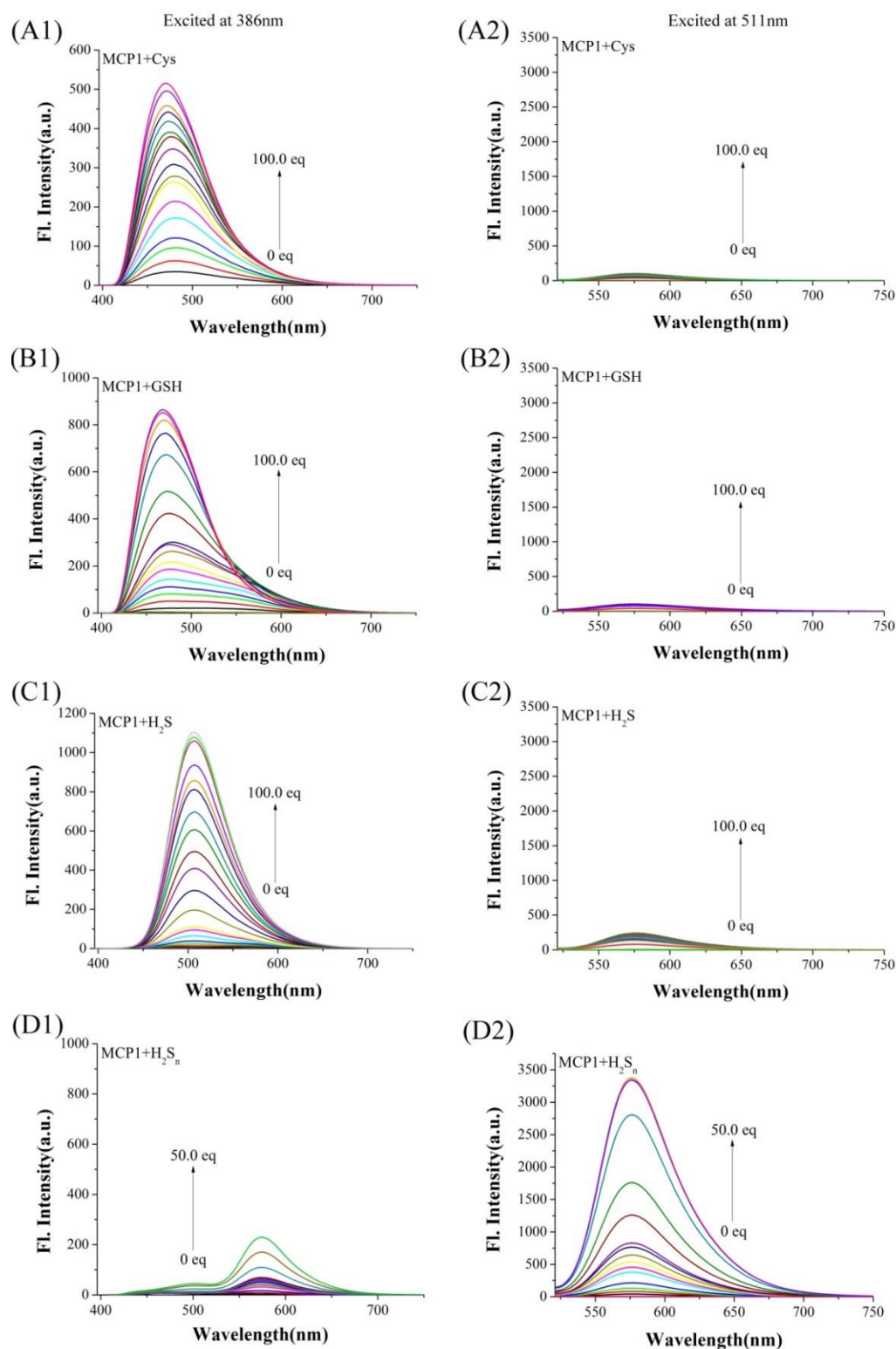


Fig. S16 Fluorescence spectra of **MCP1** (10 μM) after the addition of incremental dose of (A) Cys (0-100.0 equiv); (B) GSH (0-100.0 equiv); (C) H_2S (0-100.0 equiv); (D) H_2S_n (0-50.0 equiv) in PBS buffer (10 mM, pH 7.4, mixed with 20% DMSO). (A1-D1) (excited at 386 nm, excitation and emission slits: 2.5/5.0 nm) in PBS buffer (10 mM, pH 7.4) at 25 $^\circ\text{C}$. (A2-D2) (excited at 511 nm, excitation and emission slits: 2.5/5.0 nm) in PBS buffer (10 mM, pH 7.4) at 25 $^\circ\text{C}$.

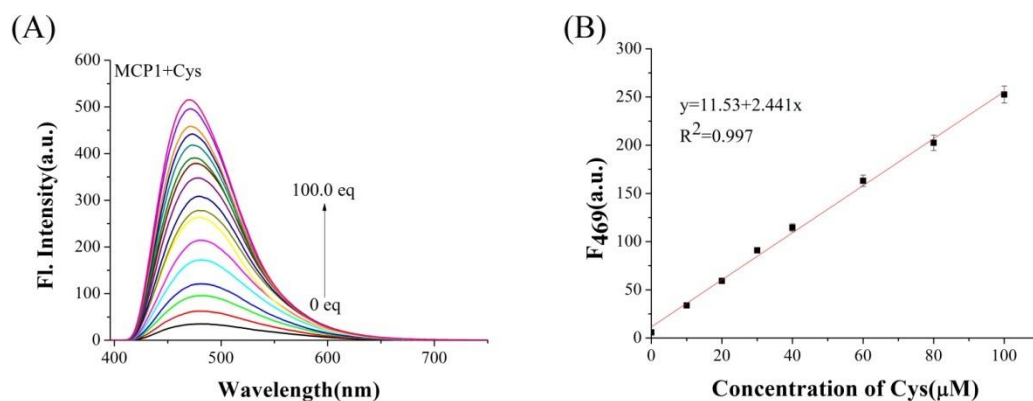


Fig. S17 Fluorescence spectra of MCP1 (10 μM) after the addition of incremental dose of (A) Cys (0-100.0 equiv) in PBS buffer (10 mM, pH 7.4, mixed with 20% DMSO) at 25 $^{\circ}\text{C}$. (B) Plot of Fluorescence intensities at 469 nm versus the concentrations of Cys. Inset: corresponding linearity.

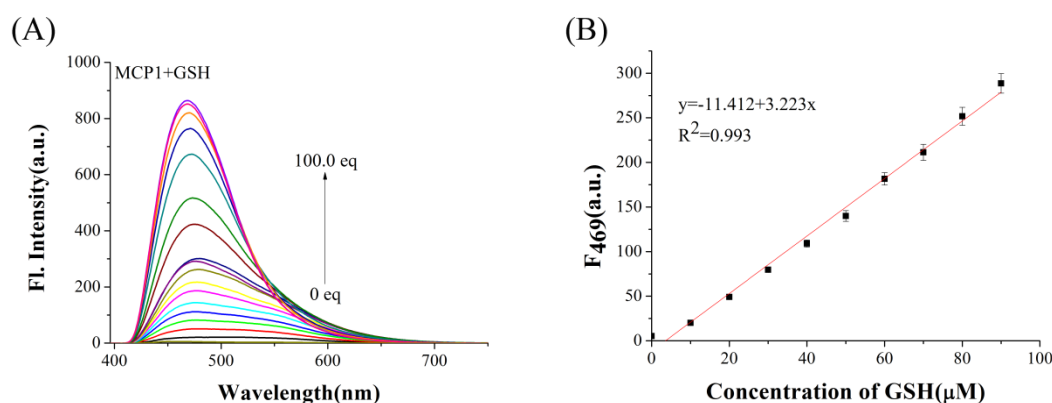


Fig. S18 Fluorescence spectra of MCP1 (10 μM) after the addition of incremental dose of (A) GSH (0-100.0 equiv) in PBS buffer (10 mM, pH 7.4, mixed with 20% DMSO) at 25 $^{\circ}\text{C}$. (B) Plot of Fluorescence intensities at 469 nm versus the concentrations of GSH. Inset: corresponding the linear correlations.

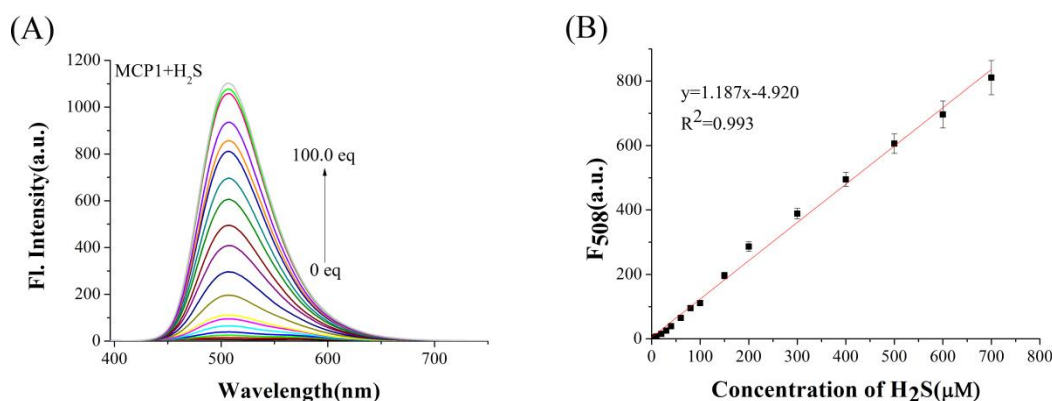


Fig. S19 Fluorescence spectra of MCP1 (10 μM) after the addition of incremental dose of (A) H_2S (0-100.0 equiv) in PBS buffer (10 mM, pH 7.4, mixed with 20% DMSO) at 25 $^{\circ}\text{C}$. (B) Plot of Fluorescence intensities at 508 nm versus the concentrations of H_2S . Inset: corresponding the linear correlations.

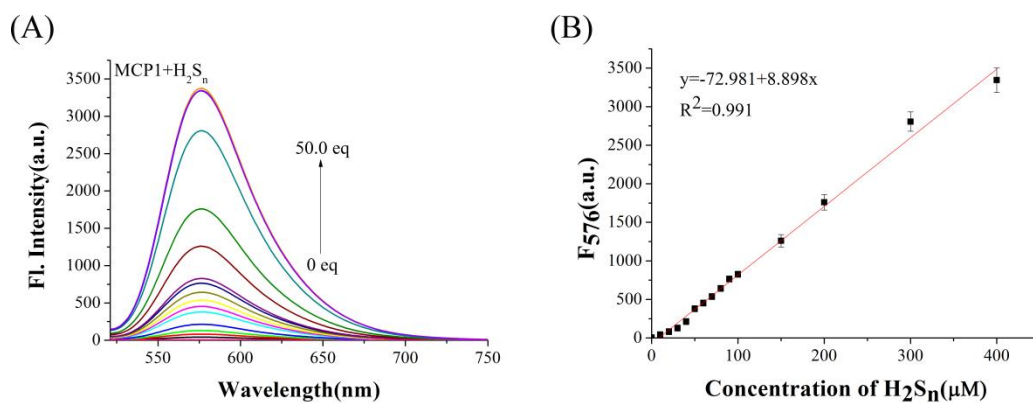


Fig. S20 Fluorescence spectra of MCP1 (10 μM) after addition of incremental dose of (A) H_2S_n (0-50.0 equiv) in PBS buffer (10 mM, pH 7.4, mixed with 20% DMSO) at 25 $^\circ\text{C}$. (B) Plot of Fluorescence intensities at 576 nm versus the concentrations of H_2S_n . Inset: corresponding the linear correlations.

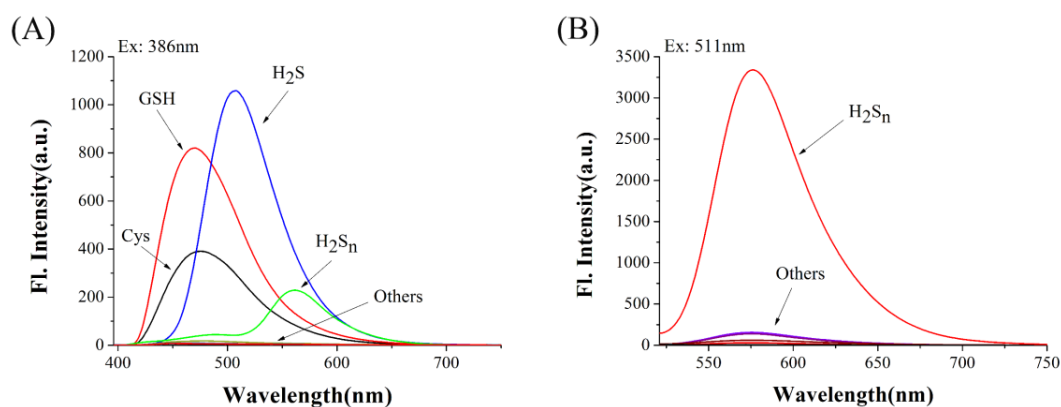


Fig. S21 Fluorescence spectra of MCP1 (10 μM) in the presence of various species (100.0 equivalents for each): H_2S , H_2S_n , $\text{S}_2\text{O}_3^{2-}$, SO_3^{2-} , SO_4^{2-} , HSO_3^- , Cys, GSH, H_2O_2 , ClO^- , O_2^- , NO, NO_2^- , NO_3^- , Ca^{2+} , K^+ , Mg^{2+} , Zn^{2+} , Ala, Arg, Asp, Lys, Met, Tyl, Gly, Glu, His, Iso, Phe, Pro, Ser, Thr, Val.

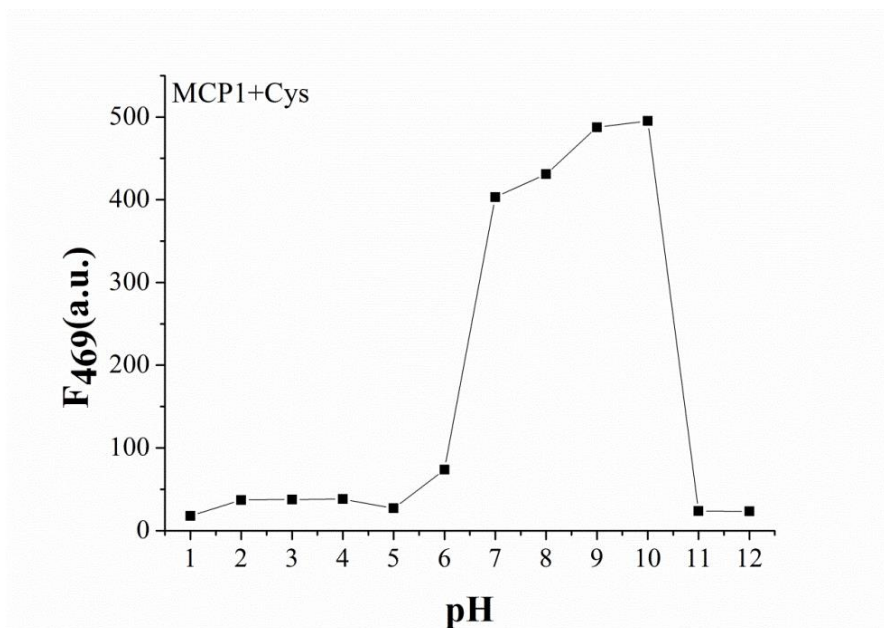


Fig. S22 pH-dependent fluorescence intensity of MCP1 (10 μ M) toward Cys (100.0 equiv), (excited at 386 nm, excitation and emission slits: 2.5/5.0 nm) in PBS buffer (10 mM, pH 1-12, mixed with 20% DMSO) at 25 $^{\circ}$ C.

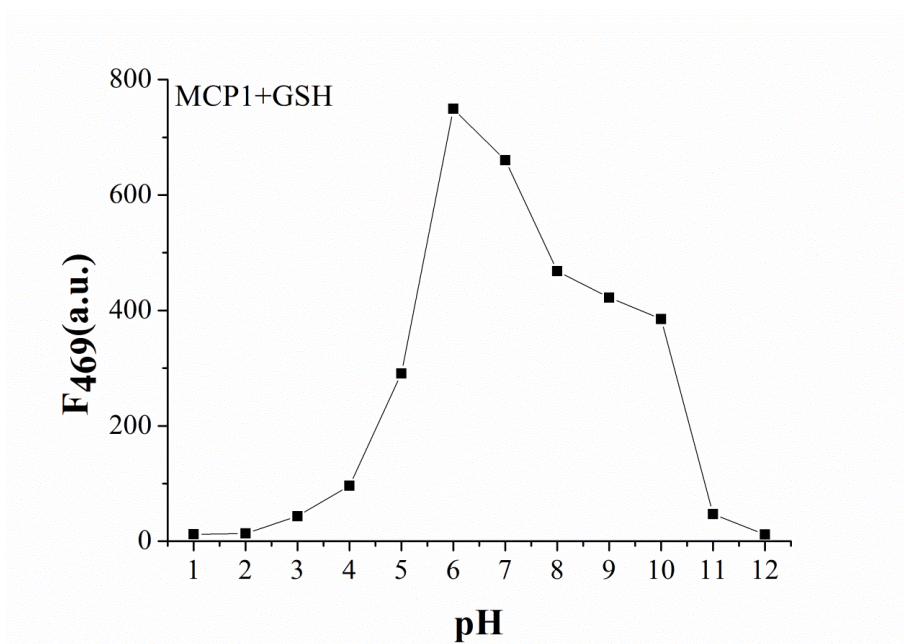


Fig. S23 pH-dependent fluorescence intensity ratio changes of MCP1 (10 μ M) toward GSH (100.0 equiv), (excited at 386 nm, excitation and emission slits: 2.5/5.0 nm) in PBS buffer (10 mM, pH 1-12, mixed with 20% DMSO) at 25 $^{\circ}$ C.

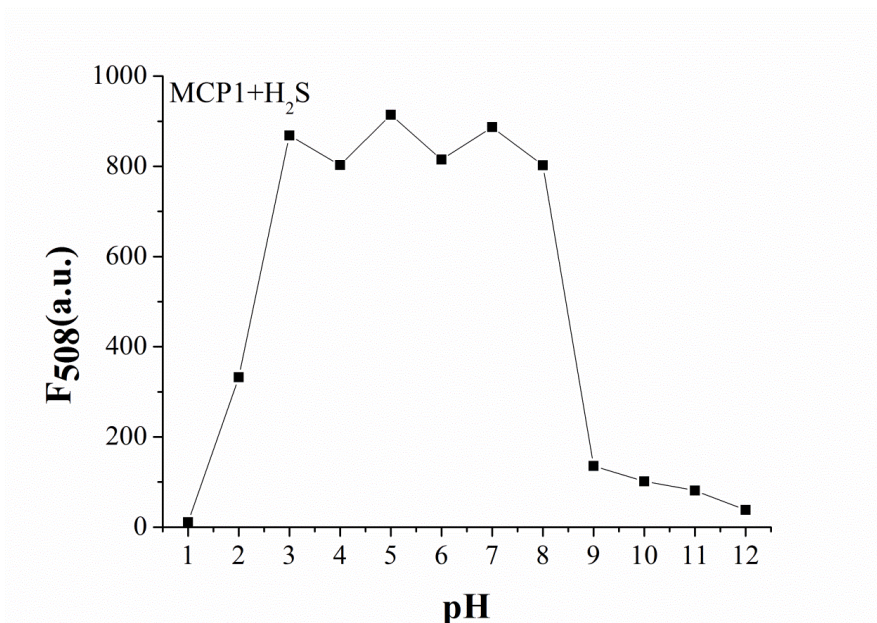


Fig. S24 pH-dependent fluorescence intensity ratio changes of MCP1 (10 μ M) toward H₂S (100.0 equiv), (excited at 386 nm, excitation and emission slits: 2.5/5.0 nm) in PBS buffer (10 mM, pH 1-12, mixed with 20% DMSO) at 25 °C.

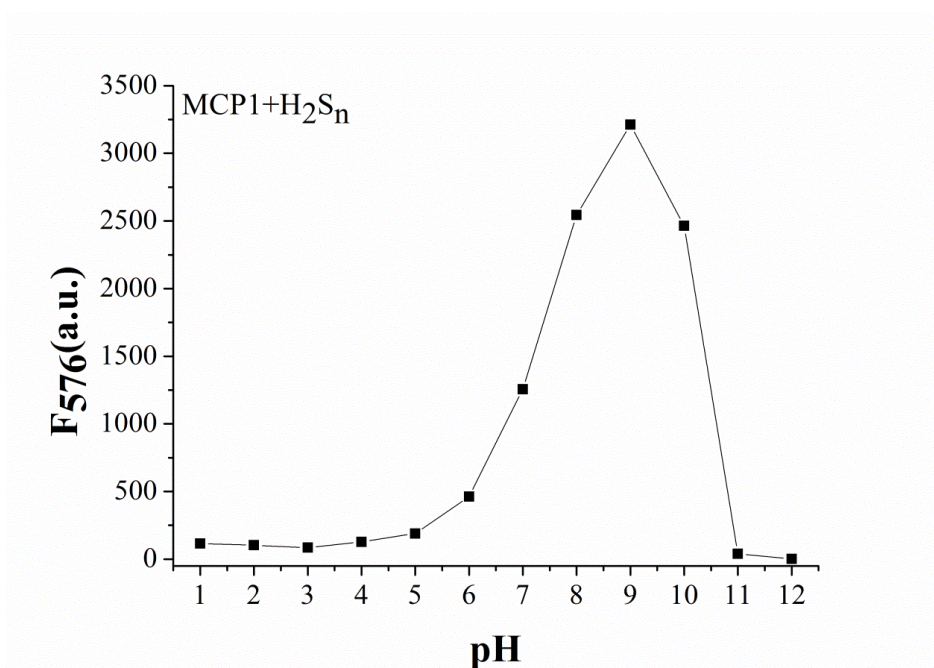


Fig. S25 pH-dependent fluorescence intensity ratio changes of MCP1 (10 μ M) toward H₂S_n (100.0 equiv), (excited at 511 nm, excitation and emission slits: 2.5/5.0 nm) in PBS buffer (10 mM, pH 1-12, mixed with 20% DMSO) at 25 °C.

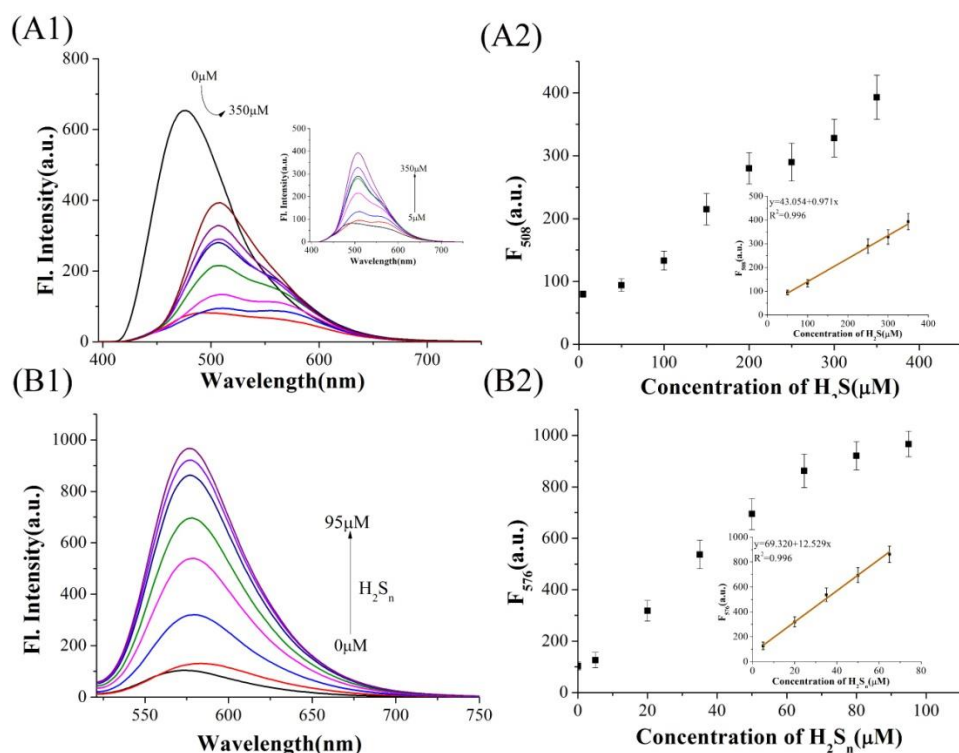


Fig. S26 Fluorescence spectra of MCP1 (10 μM) after the addition of incremental dose of H₂S (0-350 μM) (A1); H₂S_n (0-95 μM) (B1) in PBS buffer (10 mM, pH 7.4, mixed with 20% DMSO) with 10 mM GSH co-existence at 25 °C. Plot of Fluorescence intensities at 508 nm versus the concentrations of H₂S (A2); 576 nm versus the concentrations of H₂S_n (B2). Inset: corresponding the linear correlations.

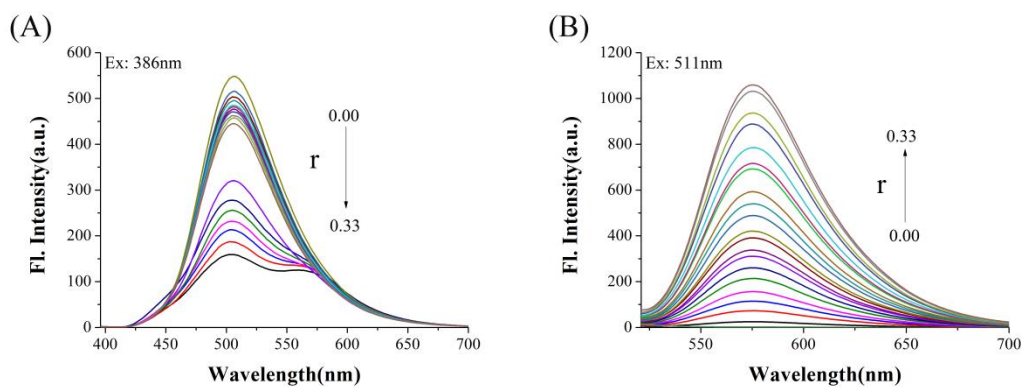


Fig. S27 Fluorescence spectra of MCP1 (10 μM) with varying H₂S_n/H₂S mixture solutions ($[H_2S_n]/[H_2S]$ (r) were 0-0.33).

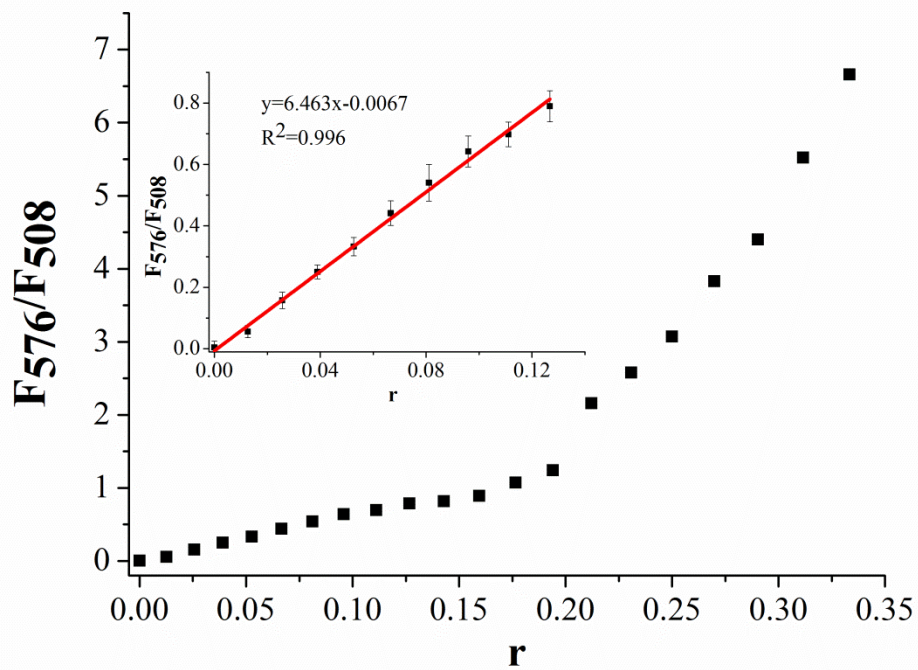


Fig. S28 Plot of Fluorescence intensity ratios F_{576}/F_{508} versus the ratios of $[H_2S_n]/[H_2S]$ (r). Inset: corresponding the linear correlations.

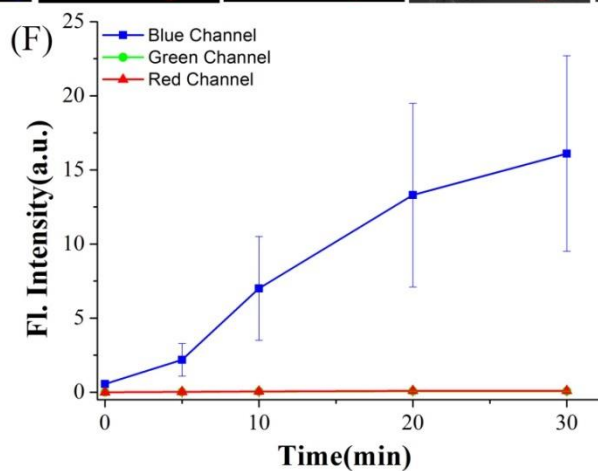
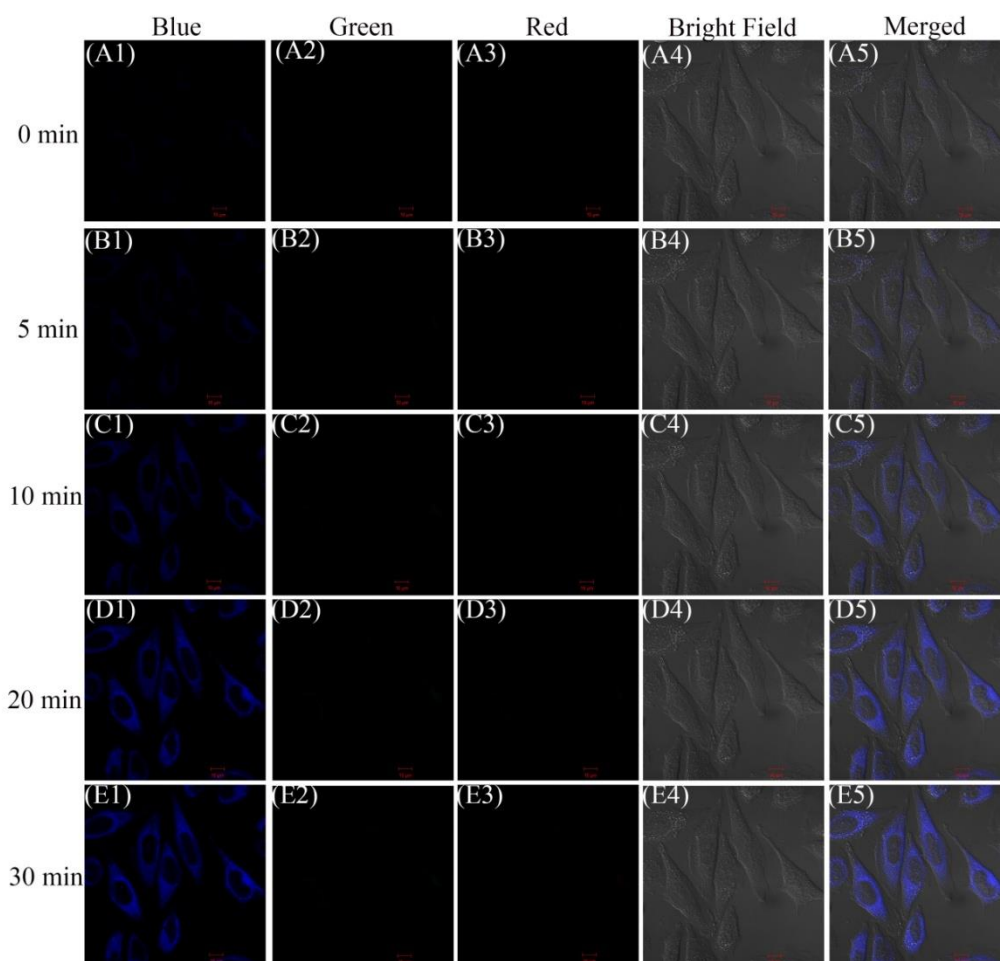


Fig. S29 Fluorescence images of HeLa cells. (A-E): Cells incubated with **MCP1** (5 μ M) for 0-30 min. Emission was collected at 420-470 nm for blue channel, 520-550 nm for green channel (both channels were excited at 405 nm), and 580-650 nm for red channel (excited at 488 nm). Scale bar: 10 μ m. (F) Time-dependent fluorescence intensity changes in blue, green and red channels, respectively.

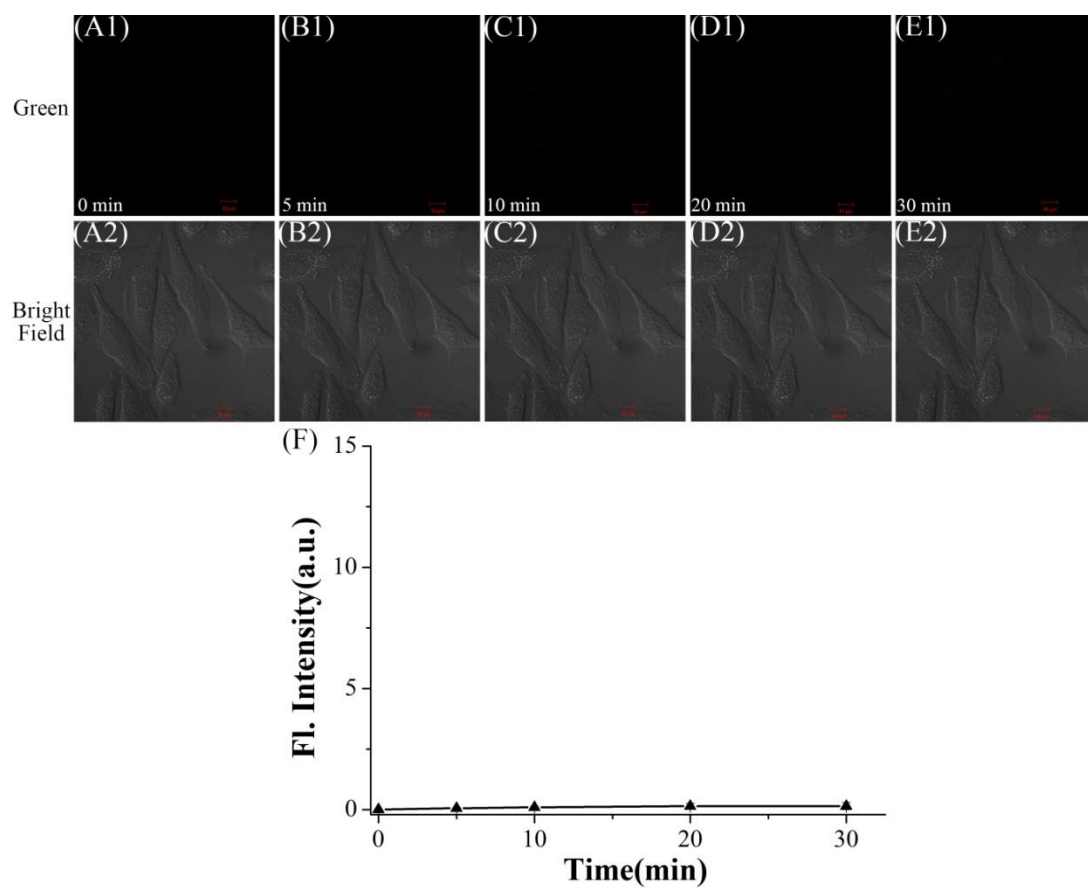


Fig. S30 Fluorescence images of HeLa cells. (A1-E1): Cells incubated with **MCP1** (5 μ M) for 0-30 min. Emission was collected at 520-550 nm for green channel (excited at 405 nm). Scale bar: 10 μ m. (A2-E2): Bright field images. (F) Time-dependent fluorescence intensity changes of green channel.

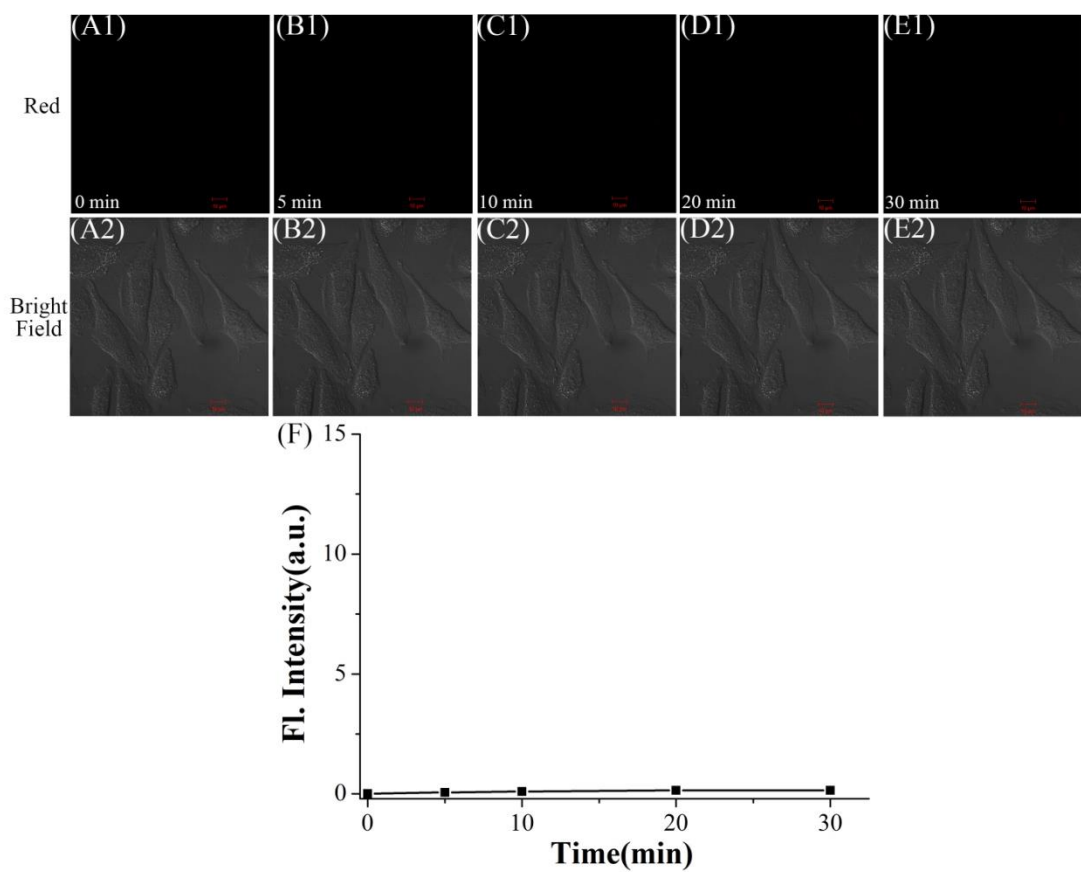


Fig. S31 Fluorescence images of HeLa cells. (A1-E1): Cells incubated with **MCP1** (5 μ M) for 0-30 min. Emission was collected at 580-650 nm for red channel (excited at 488 nm). Scale bar: 10 μ m. (A2-E2): Bright field images. (F) Time-dependent fluorescence intensity changes of red channel.

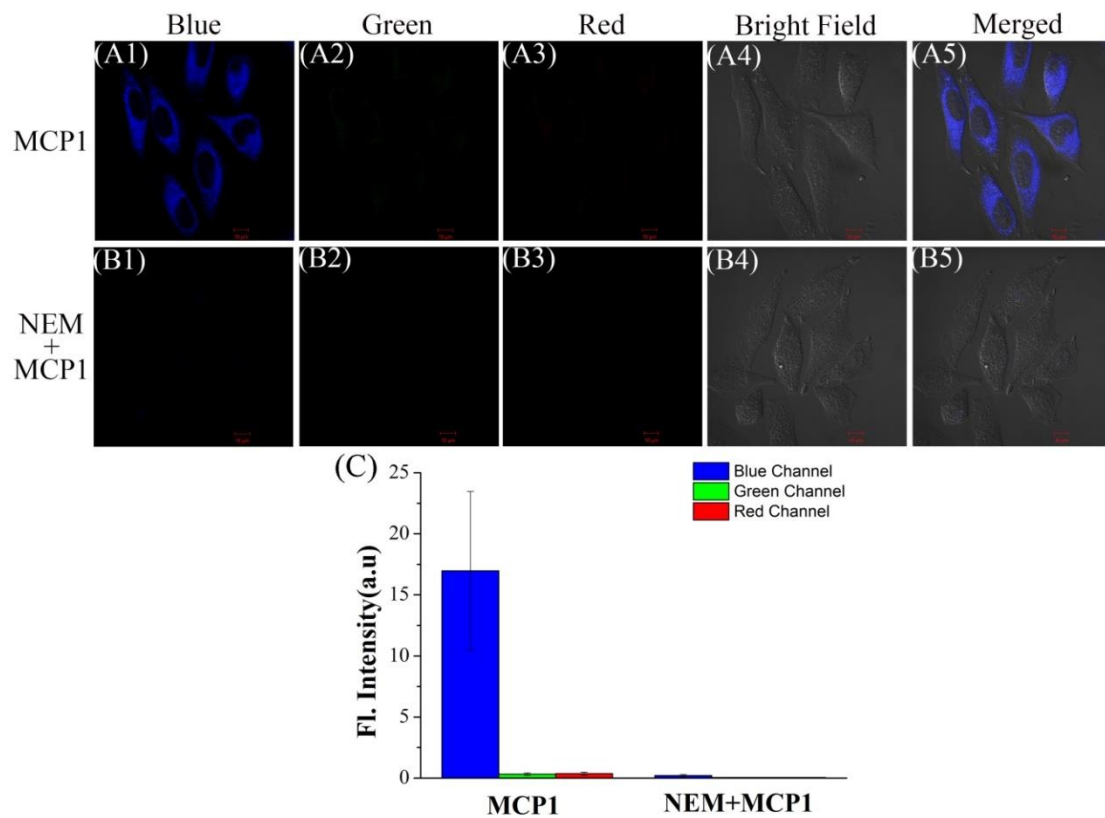


Fig. S32 Fluorescence images of HeLa cells. (A1-A5): Cells incubated with **MCP1** (5 μ M) for 15 min. (B1-B5): Cells incubated with 1 mM NEM for 15 min, and **MCP1** (5 μ M) for additional 15 min. Emission was collected at 420-470 nm for blue channel, 520-550 nm for green channel (both channels were excited at 405 nm), and 580-650 nm for red channel (excited at 488 nm). Scale bar: 10 μ m. (C) Fluorescence intensity changes of blue, green and red channels respectively.

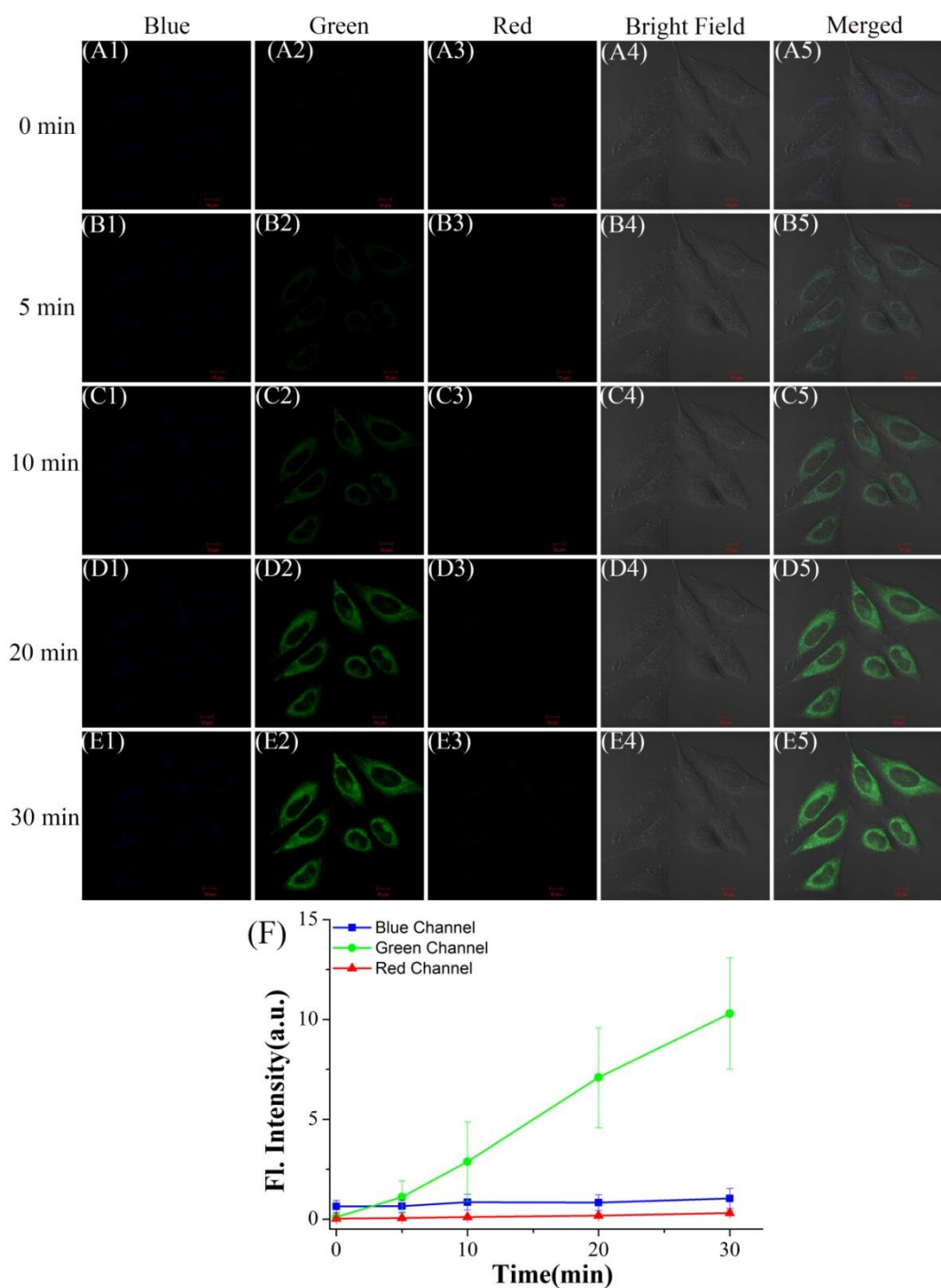


Fig. S33 Fluorescence images of HeLa cells. (A-E): Cells incubated with 100 μM H_2S for 15 min, and **MCP1** (5 μM) for additional 0-30 min. Emission was collected at 420-470 nm for blue channel, 520-550 nm for green channel (both channels were excited at 405 nm), and 580-650 nm for red channel (excited at 488 nm). Scale bar: 10 μm . (F) Time-dependent fluorescence intensity changes in blue, green and red channels, respectively.

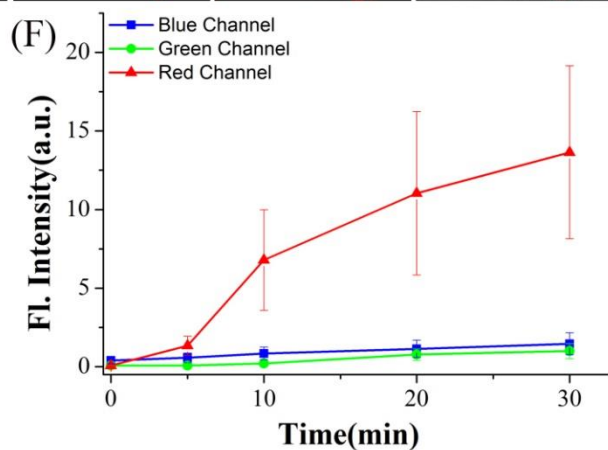
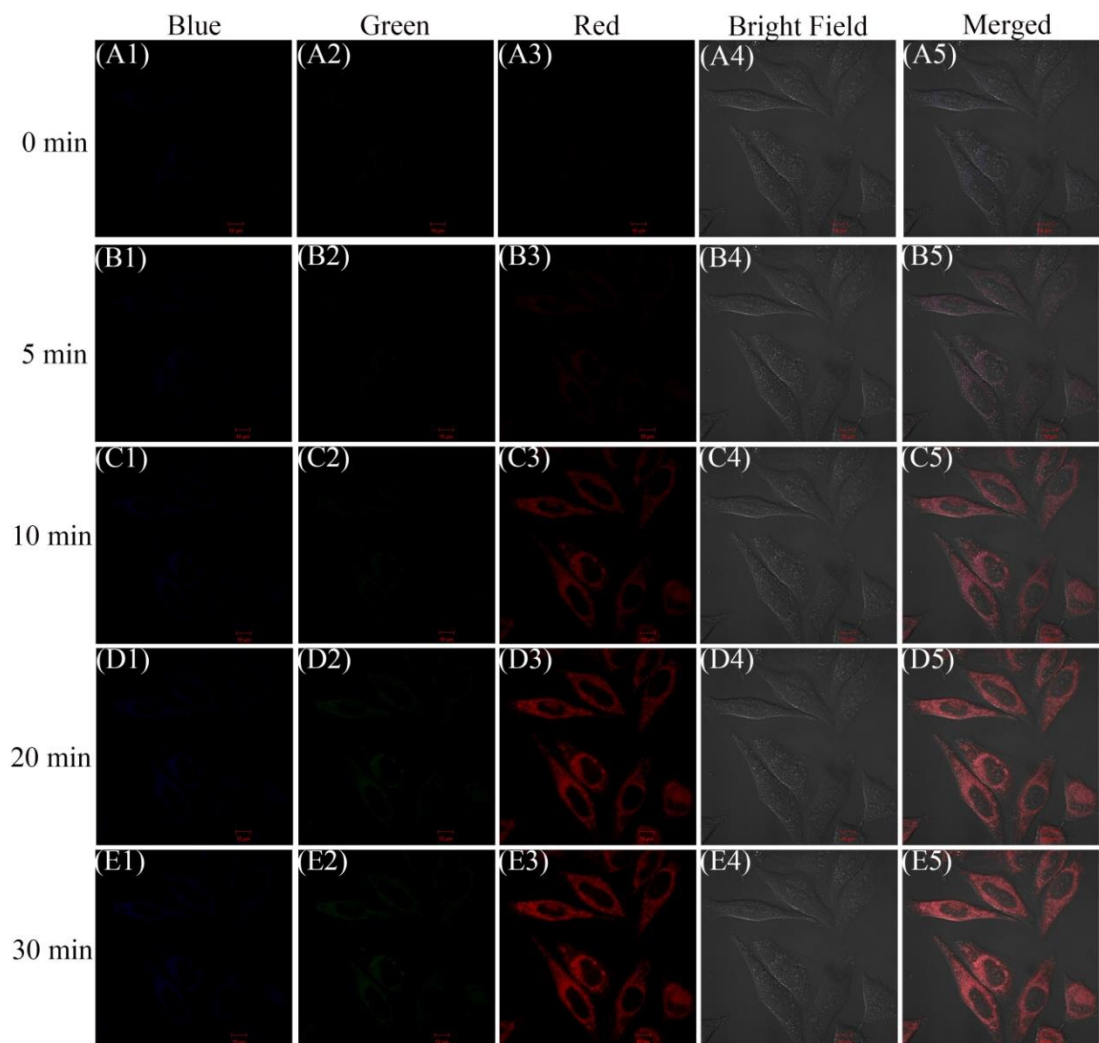


Fig. S34 Fluorescence images of HeLa cells. (A-E): Cells incubated with 200 μM H_2S_n for 15 min, and **MCP1** (5 μM) for additional 0-30 min. Emission was collected at 420-470 nm for blue channel, 520-550 nm for green channel (both channels were excited at 405 nm), and 580-650 nm for red channel (excited at 488 nm). Scale bar: 10 μm . (F) Time-dependent fluorescence intensity changes in blue, green and red channels, respectively.

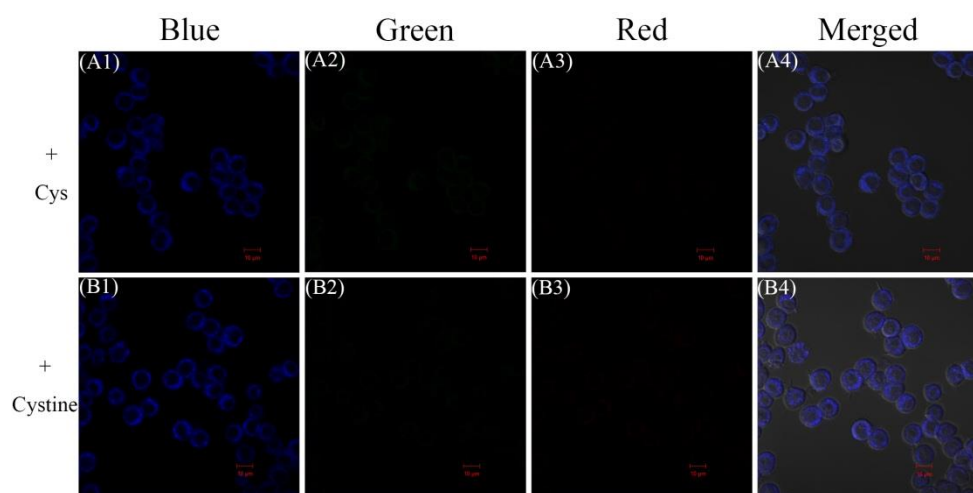


Fig. S35 (A1-A4): Cells incubated with 200 μM Cys for 30 min, 5 μM **MCP1** for additional 15 min. (B1-B4): Cells incubated with 200 μM cystine for 30 min, 5 μM **MCP1** for additional 15 min.

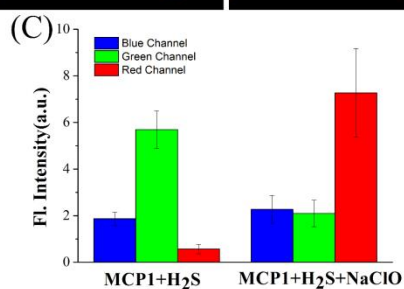
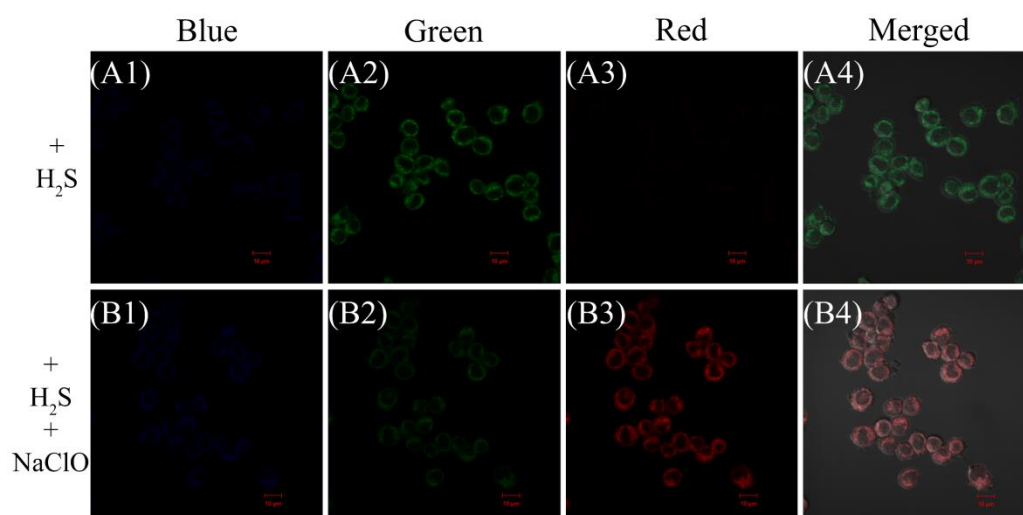


Fig. S36 Fluorescence images of RAW 264.7 cells. (A): Cells incubated with 200 μM H_2S for 15 min, and **MCP1** (5 μM) for additional 30 min. (B): Cells incubated with 200 μM H_2S and 100 μM NaClO for 15 min, and **MCP1** (5 μM) for additional 30 min. Emission was collected at 420-470 nm for blue channel, 520-550 nm for green channel (both channels were excited at 405 nm), and 580-650 nm for red channel (excited at 488 nm). Scale bar: 10 μm .

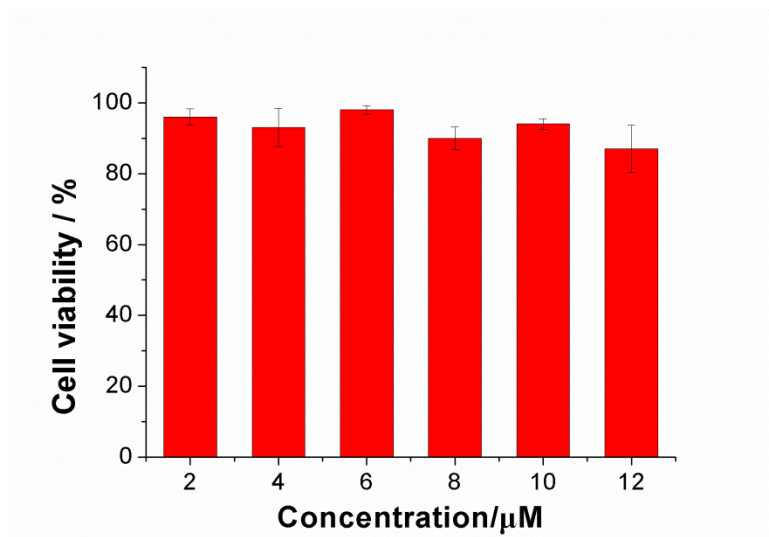


Fig. S37 Percentage of viable RAW 264.7 cells after treatment with indicated concentrations of **MCP1** after 12 hours.

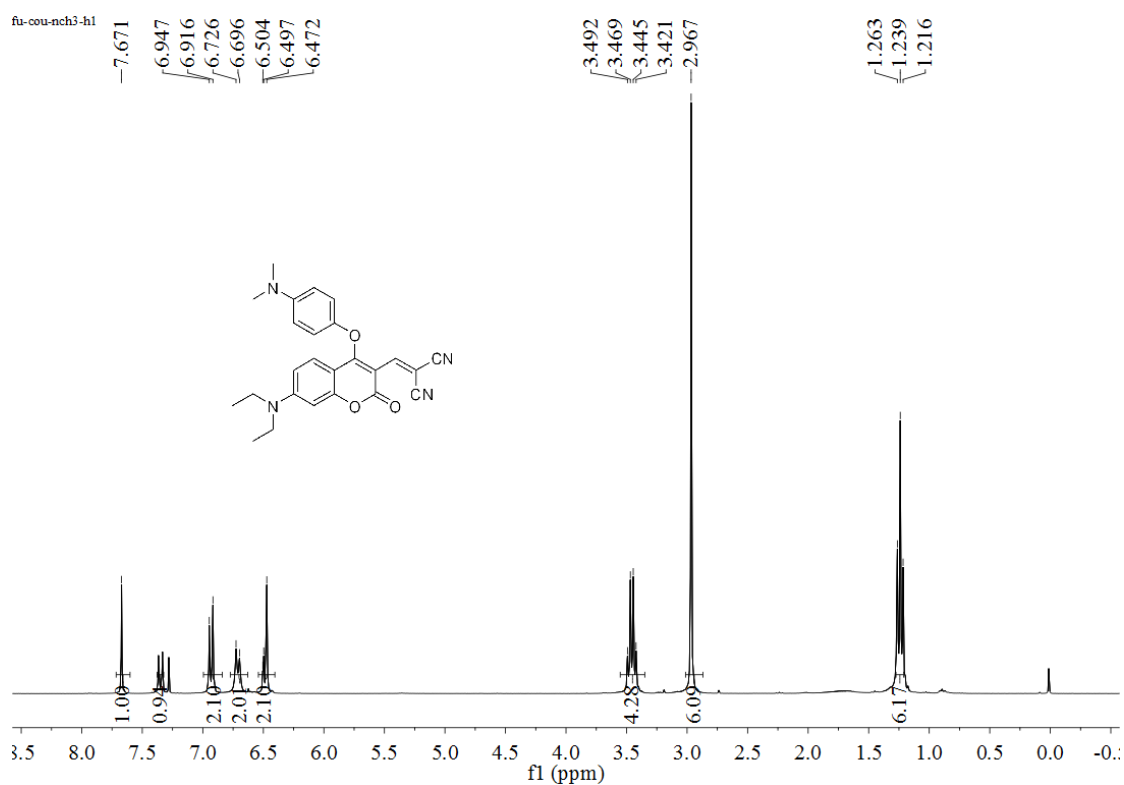


Fig. S38 ^1H NMR spectrum of **MCP1** (CDCl_3 , 300 MHz).

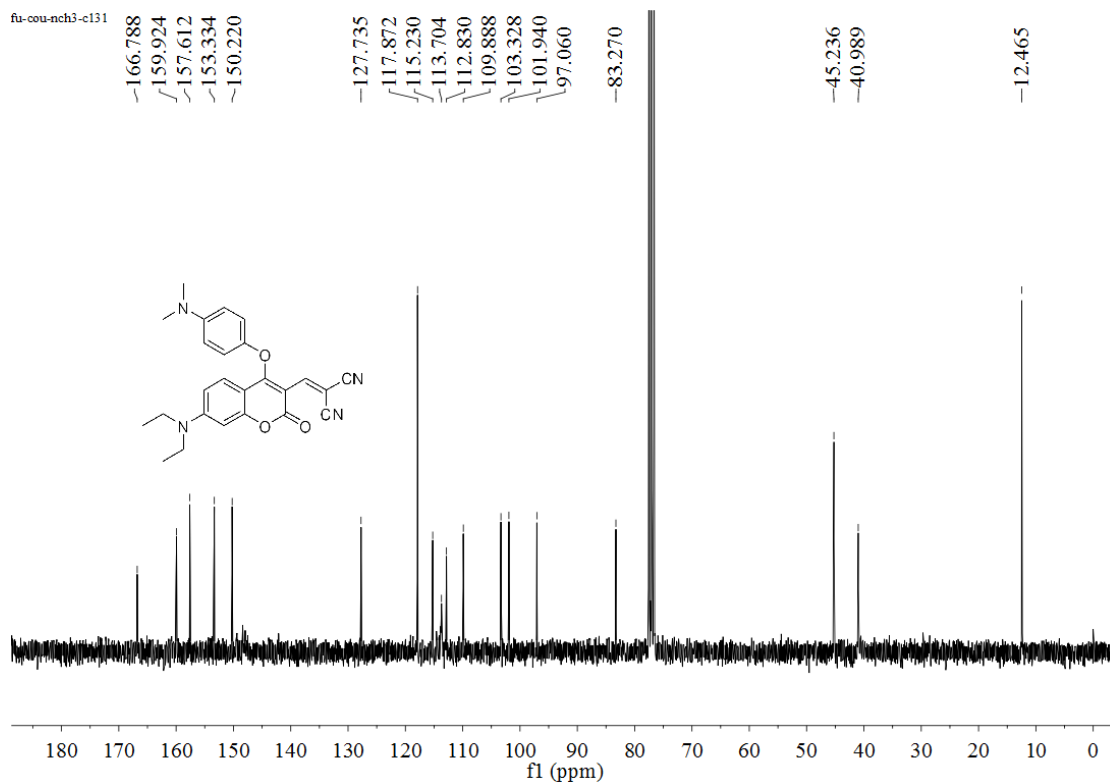


Fig. S39 ^{13}C NMR spectrum of MCP1 (CDCl_3 , 75 MHz).

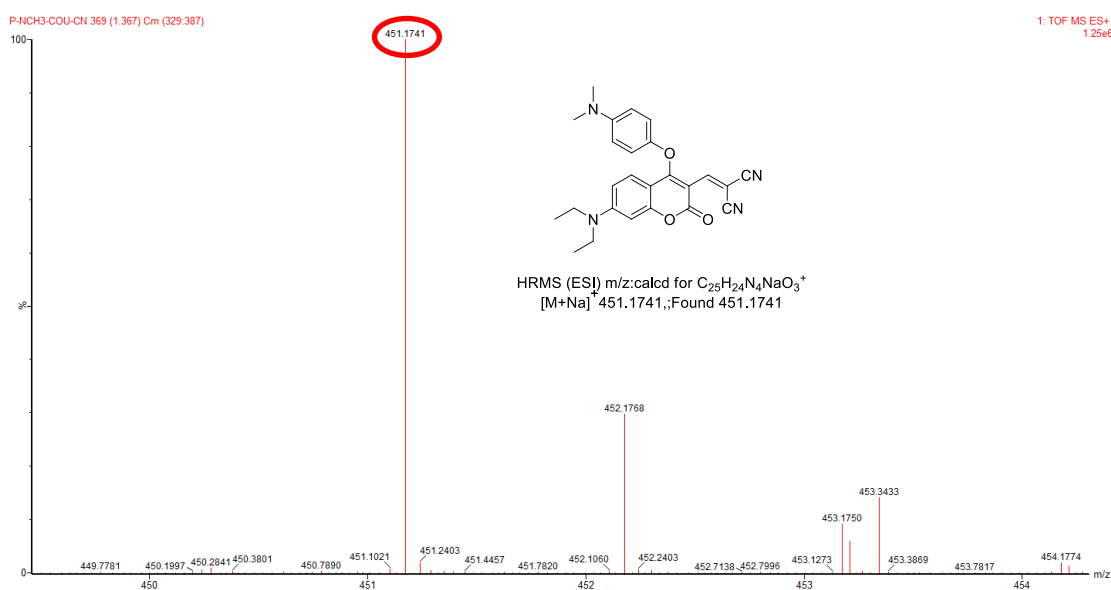


Fig. S40 HRMS spectrum of MCP1.

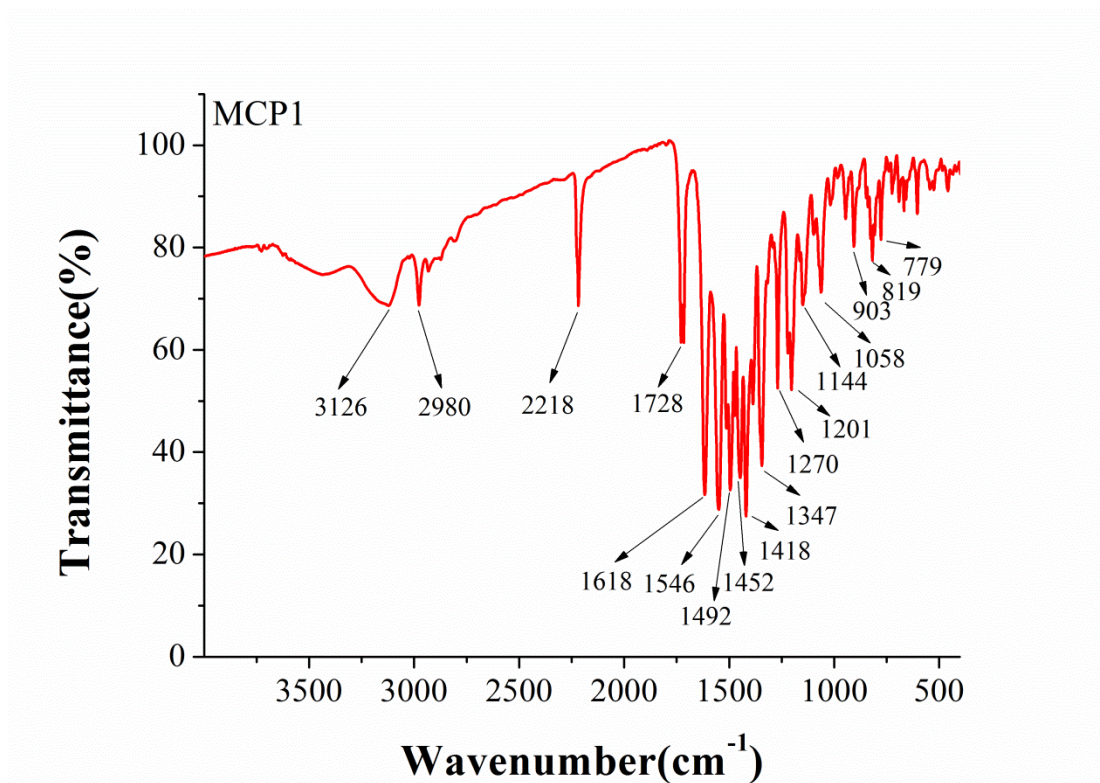


Fig. S41 FTIR spectrum of MCP1.

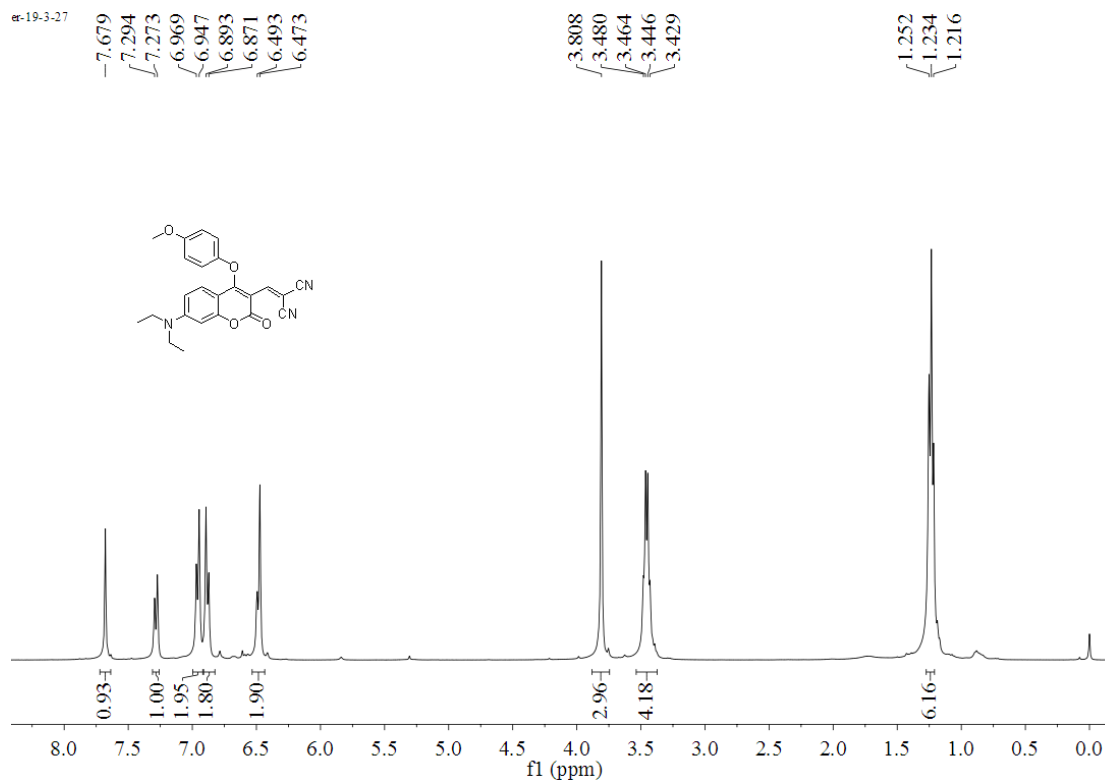


Fig. S42 ^1H NMR spectrum of MCP2 (CDCl_3 , 400 MHz).

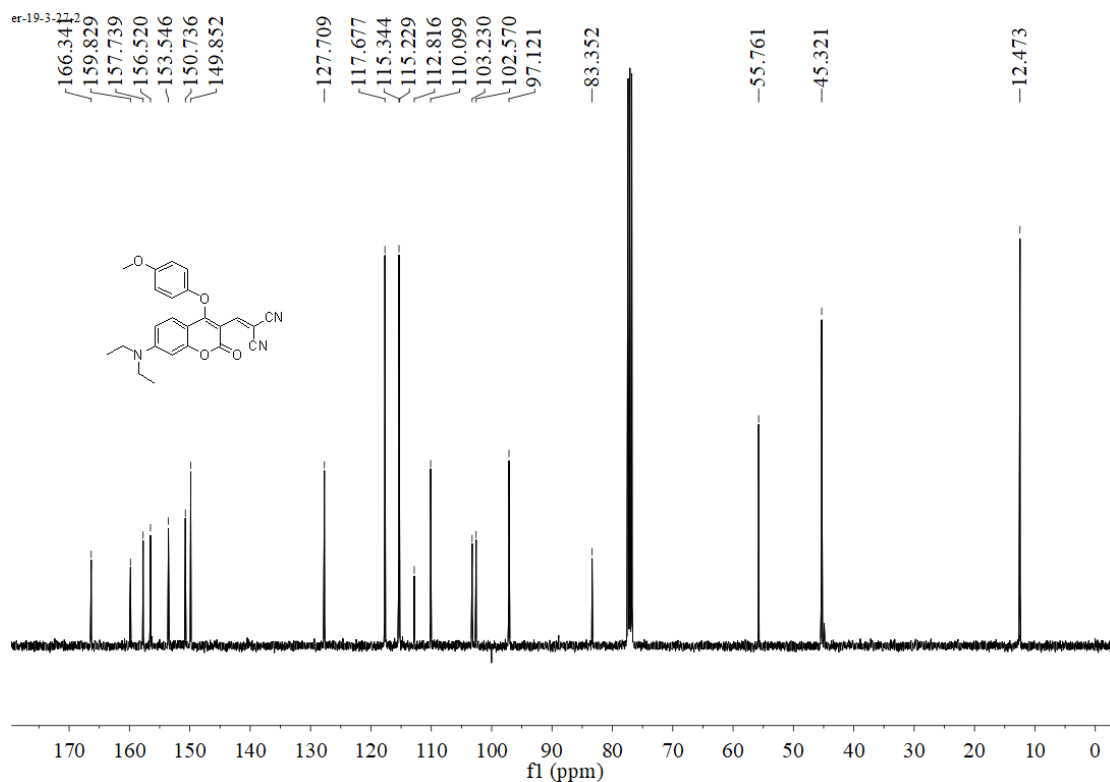


Fig. S43 ^{13}C NMR spectrum of MCP2 (CDCl_3 , 101 MHz).

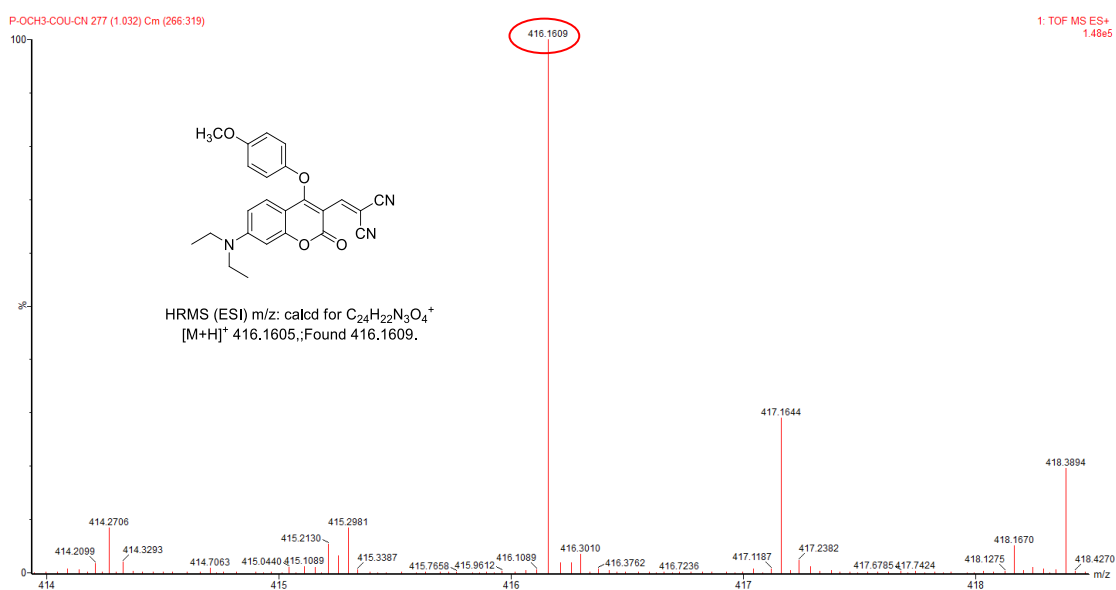


Fig. S44 HRMS spectrum of MCP2.

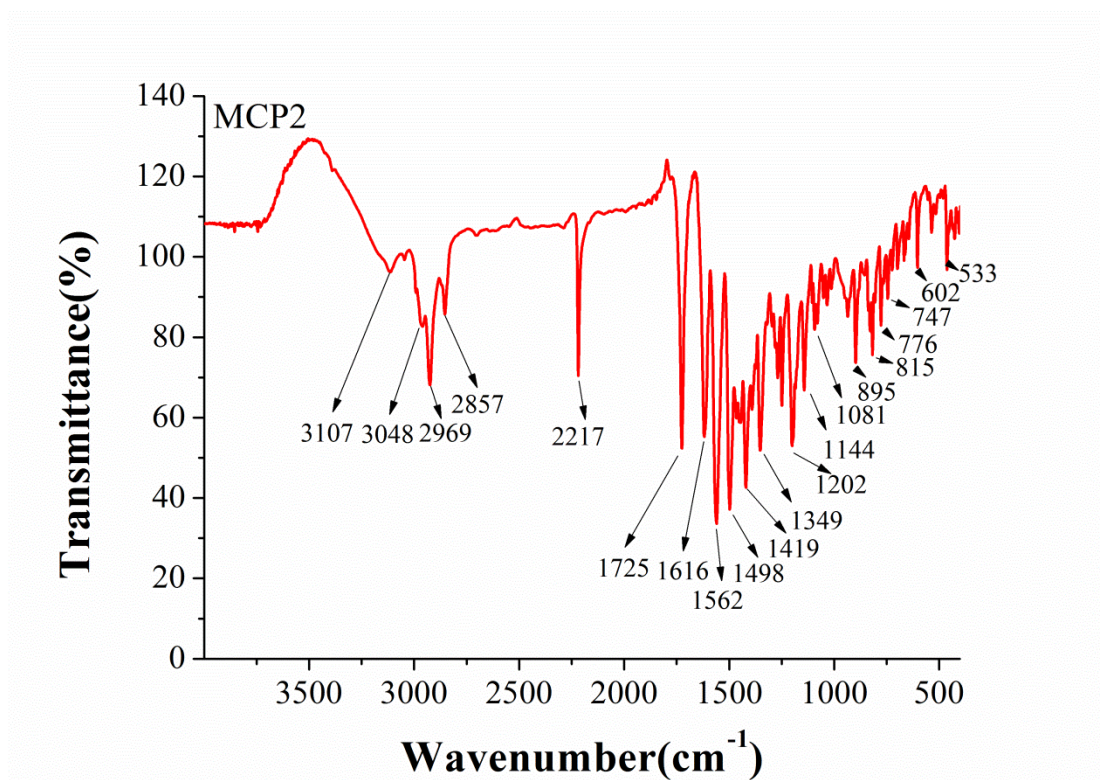


Fig. S45 FTIR spectrum of MCP2.

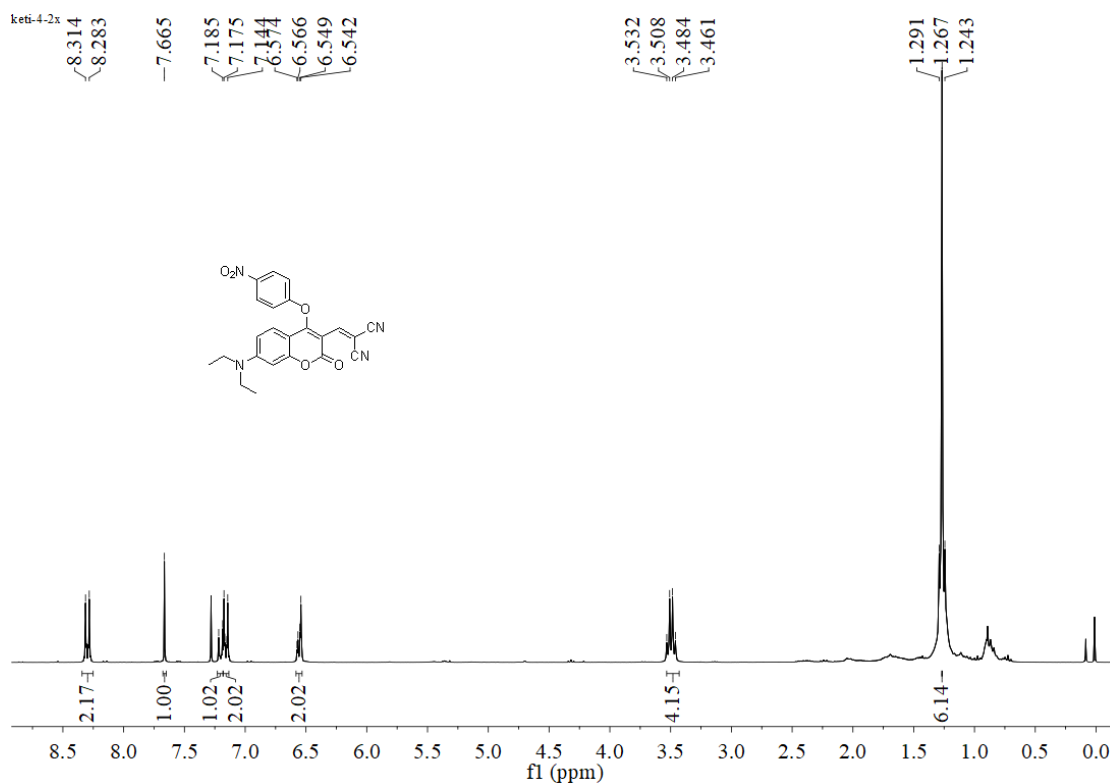


Fig. S46 ¹H NMR spectrum of MCP3 (CDCl₃, 300 MHz).

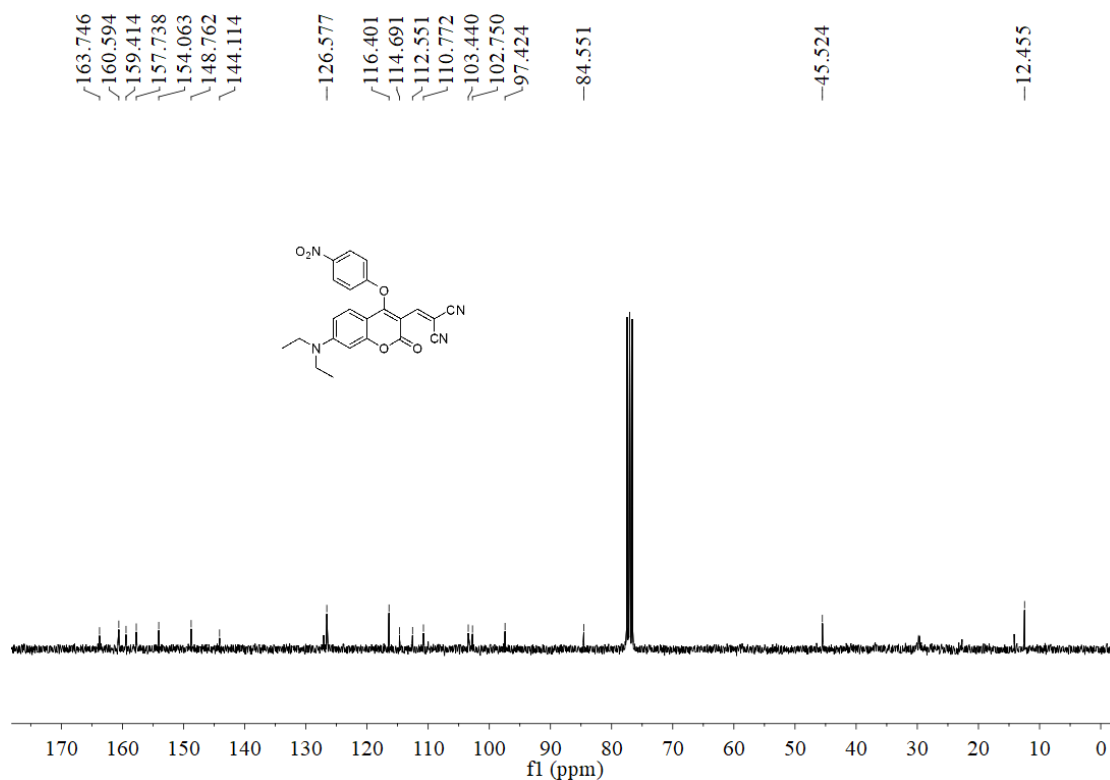


Fig. S47 ¹³C NMR spectrum of MCP3 (CDCl₃, 75 MHz).

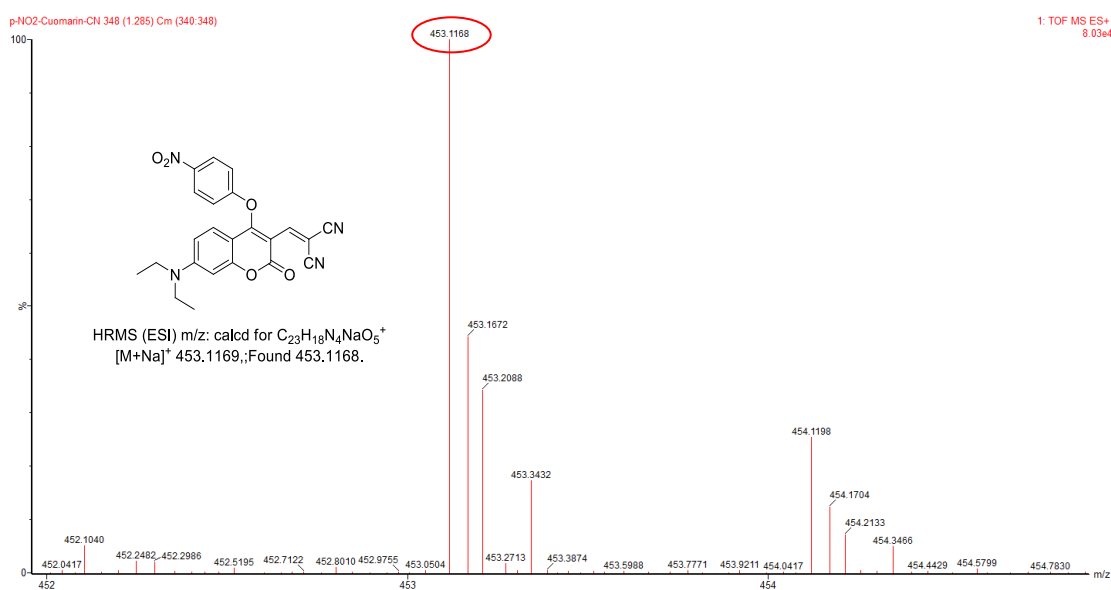


Fig. S48 HRMS spectrum of MCP3.

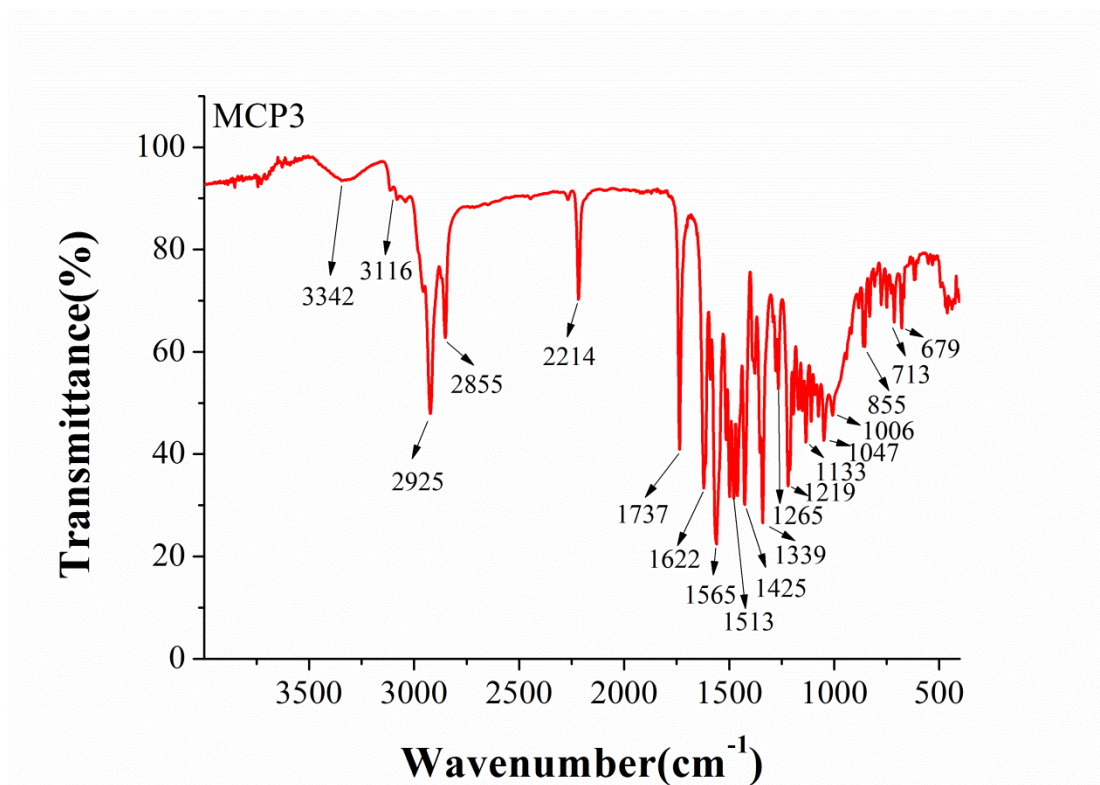


Fig. S49 FTIR spectrum of MCP3.

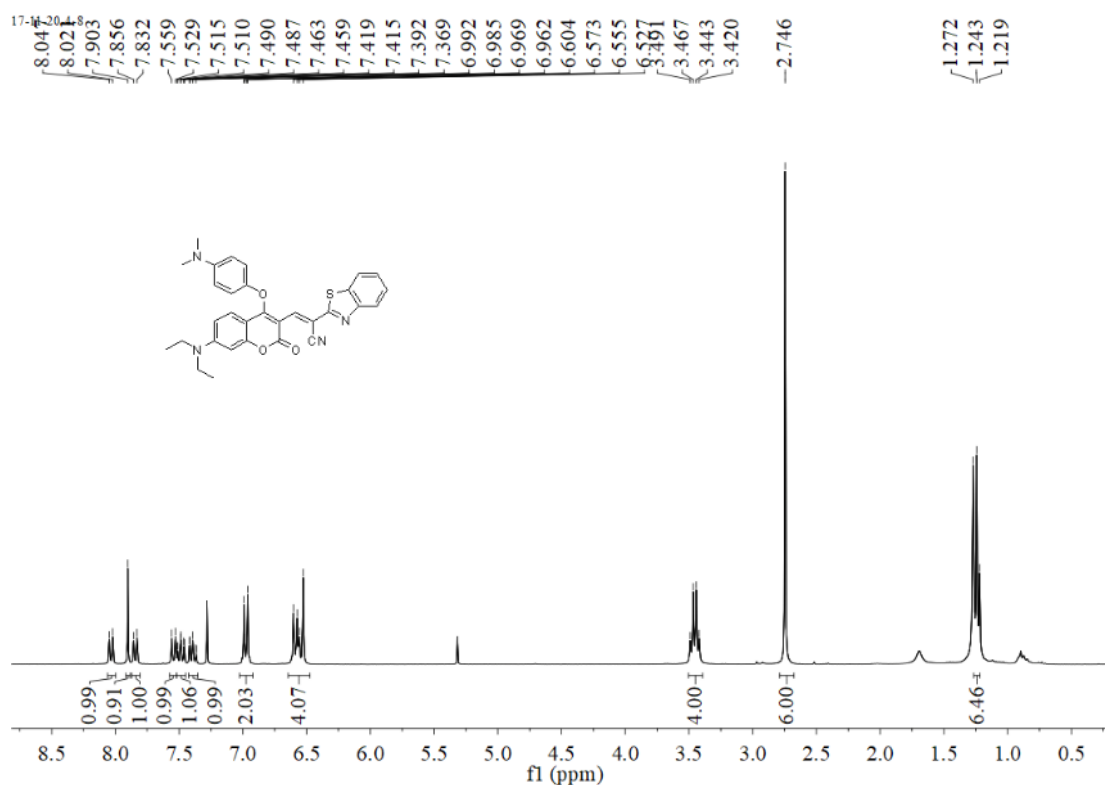


Fig. S50 ¹H NMR spectrum of MCP4 (CDCl₃, 300 MHz).

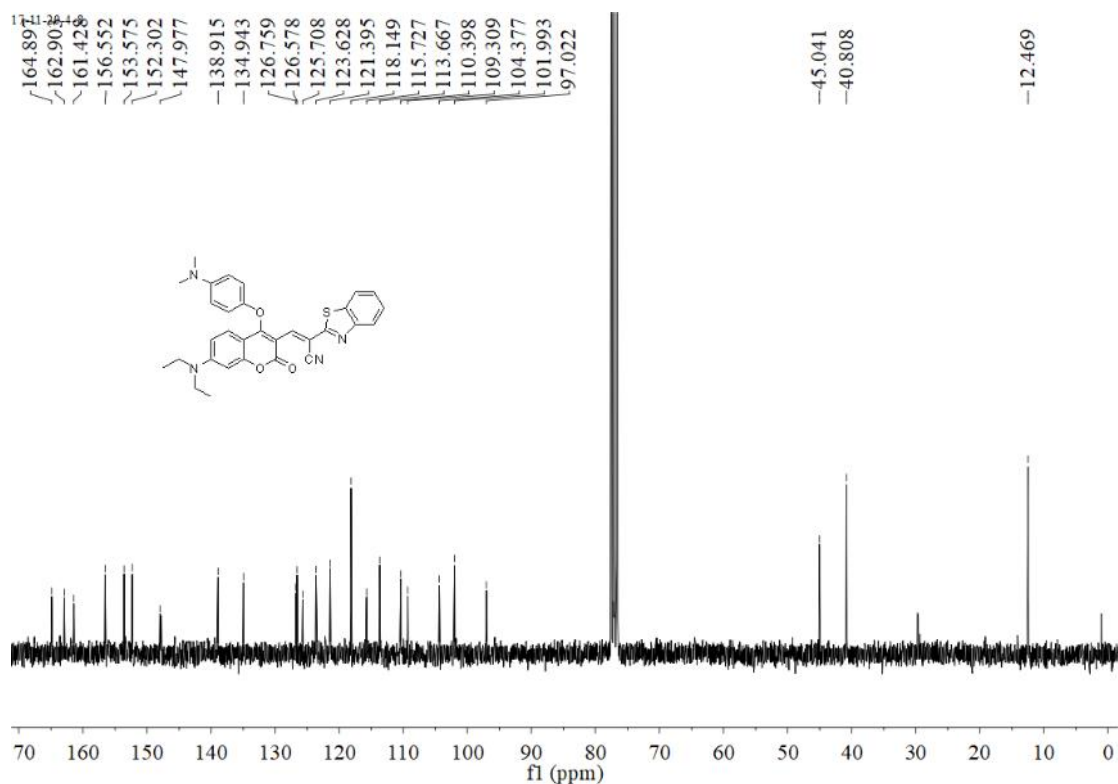


Fig. S51 ¹³C NMR spectrum of MCP4 (CDCl₃, 75 MHz).

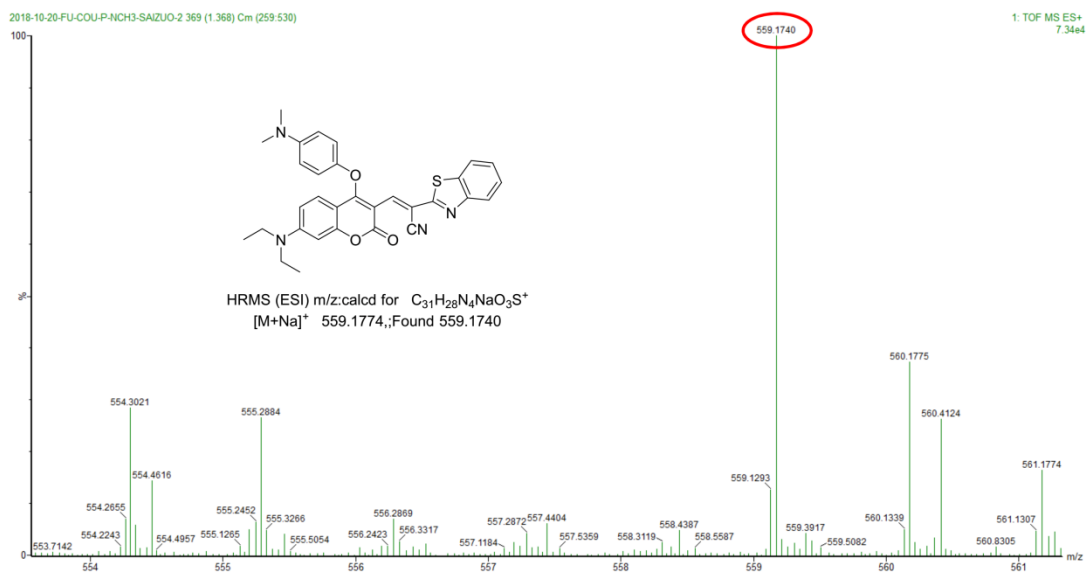


Fig. S52 HRMS spectrum of MCP4.

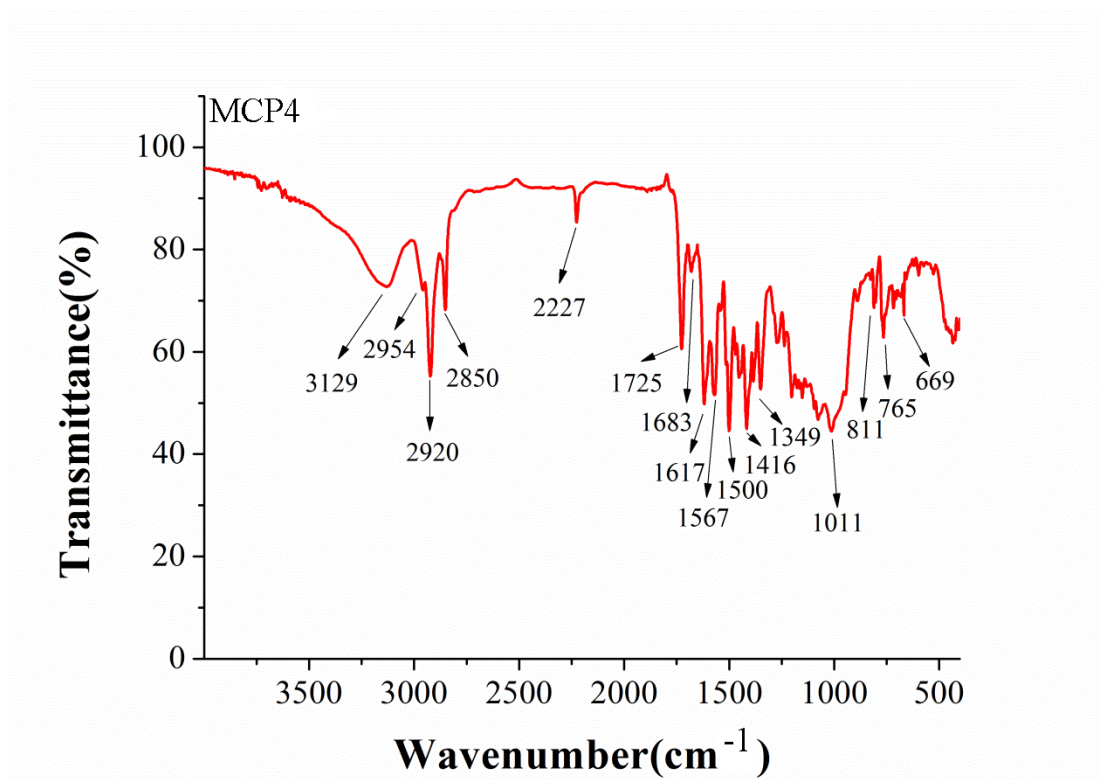


Fig. S53 FTIR spectrum of MCP4.

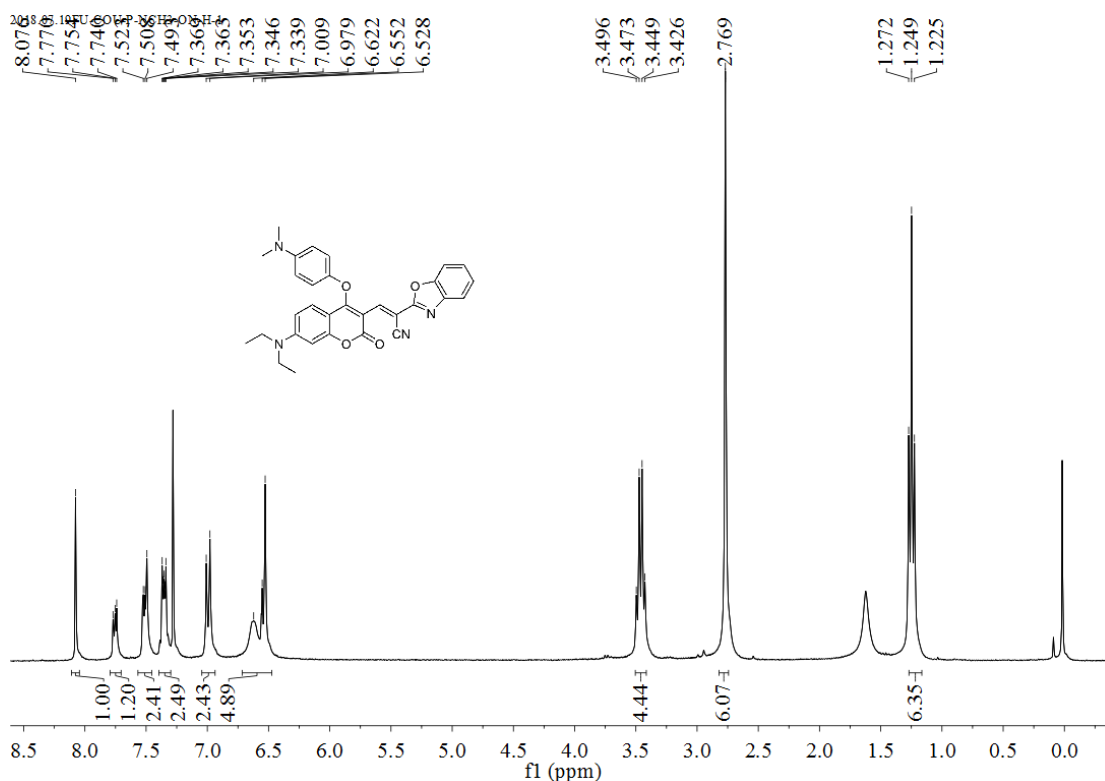


Fig. S54 ¹H NMR spectrum of MCP5 (CDCl₃, 300 MHz).

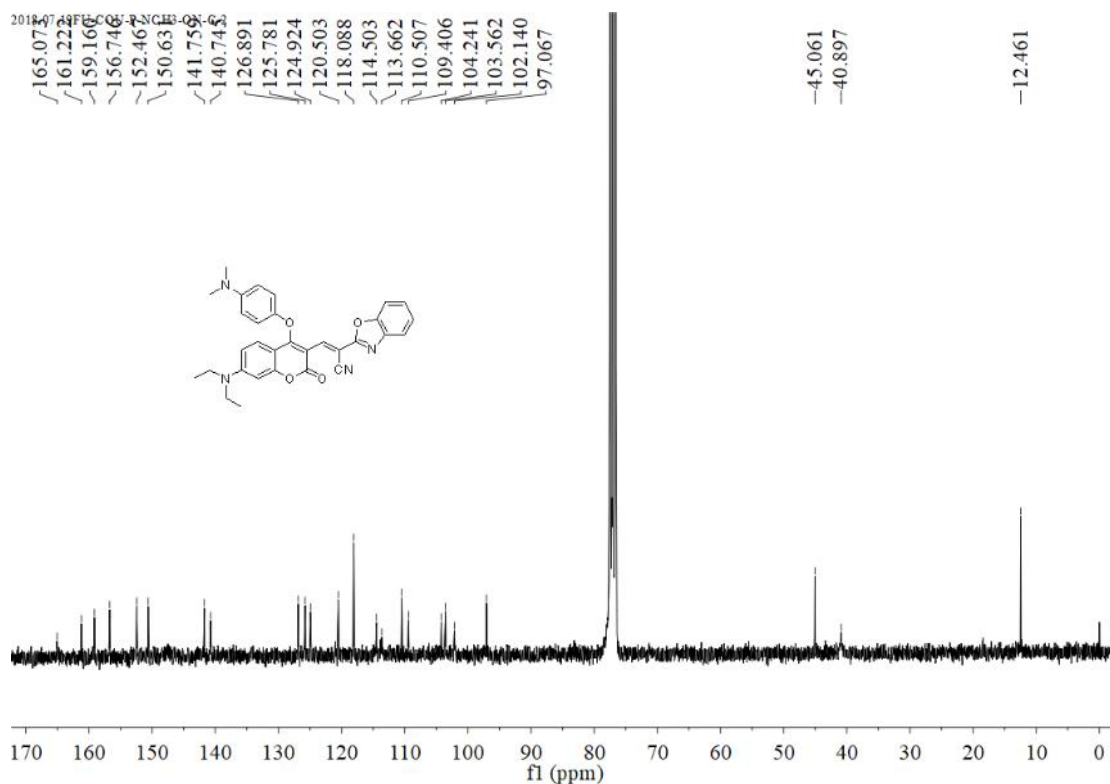


Fig. S55 ^{13}C NMR spectrum of MCP5 (CDCl_3 , 75 MHz).

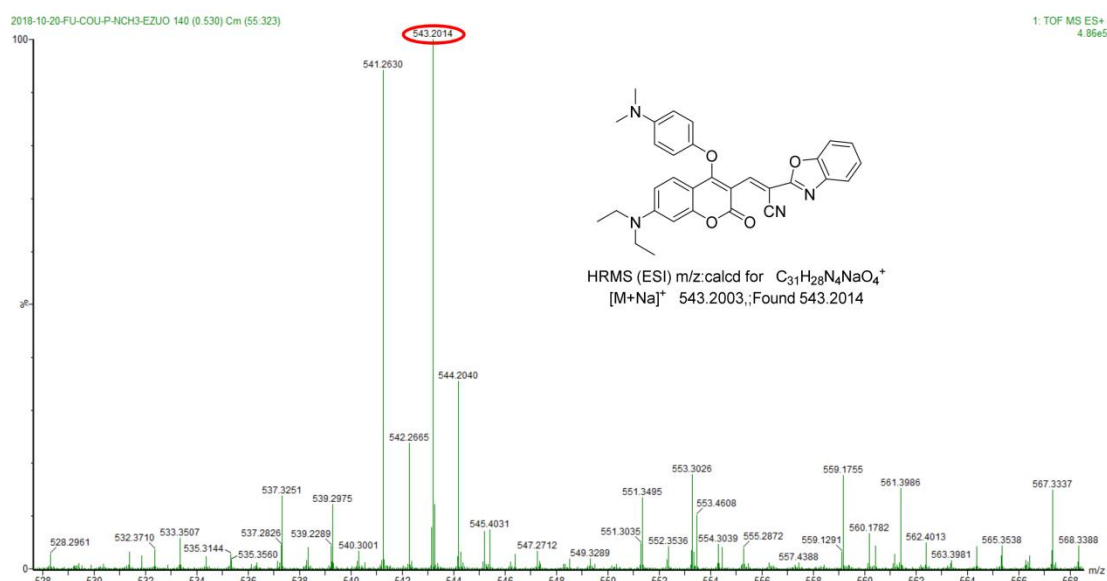


Fig. S56 HRMS spectrum of MCP5.

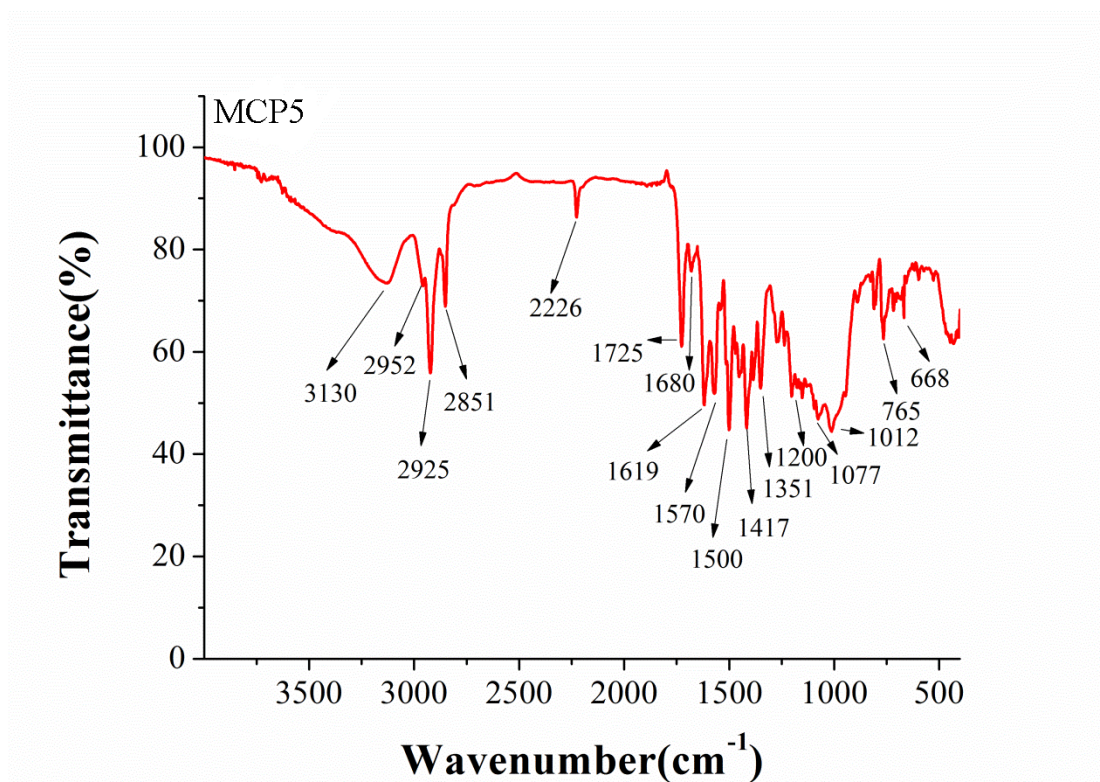


Fig. S57 FTIR spectrum of MCP5.

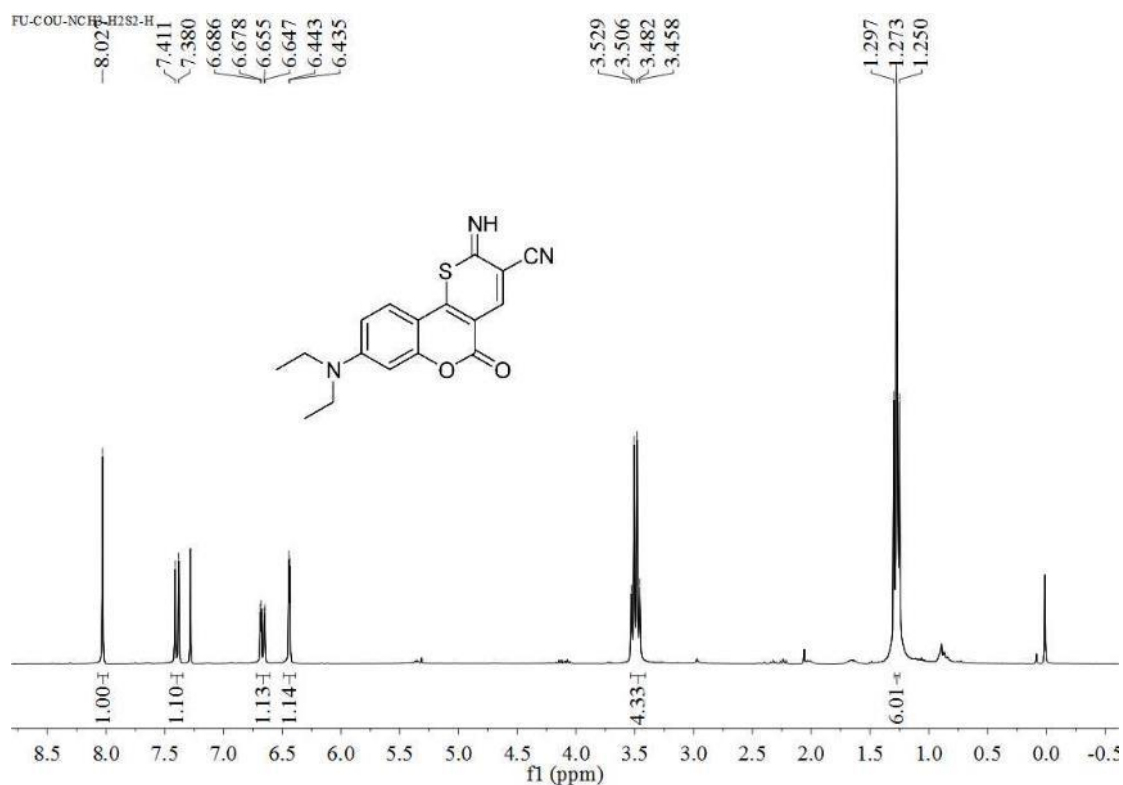


Fig. S58 ^1H NMR spectrum of **7** (CDCl_3 , 300 MHz).

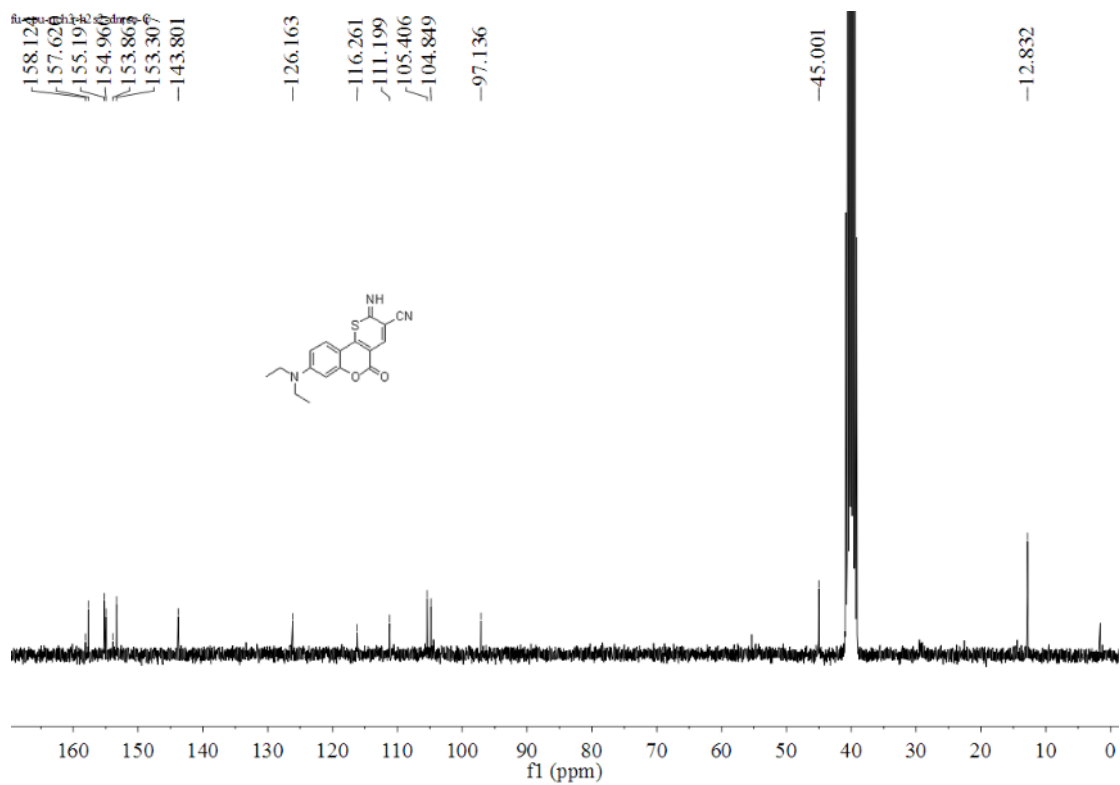


Fig. S59 ¹³C NMR spectrum of **7** (CDCl₃, 75 MHz).

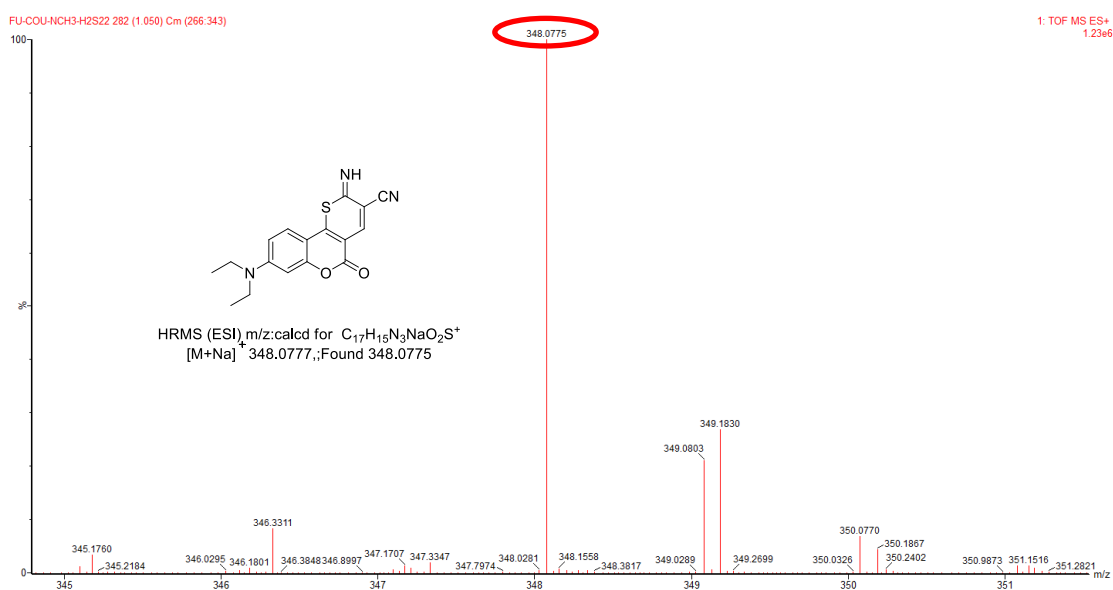


Fig. S60 HRMS spectrum of **7**.

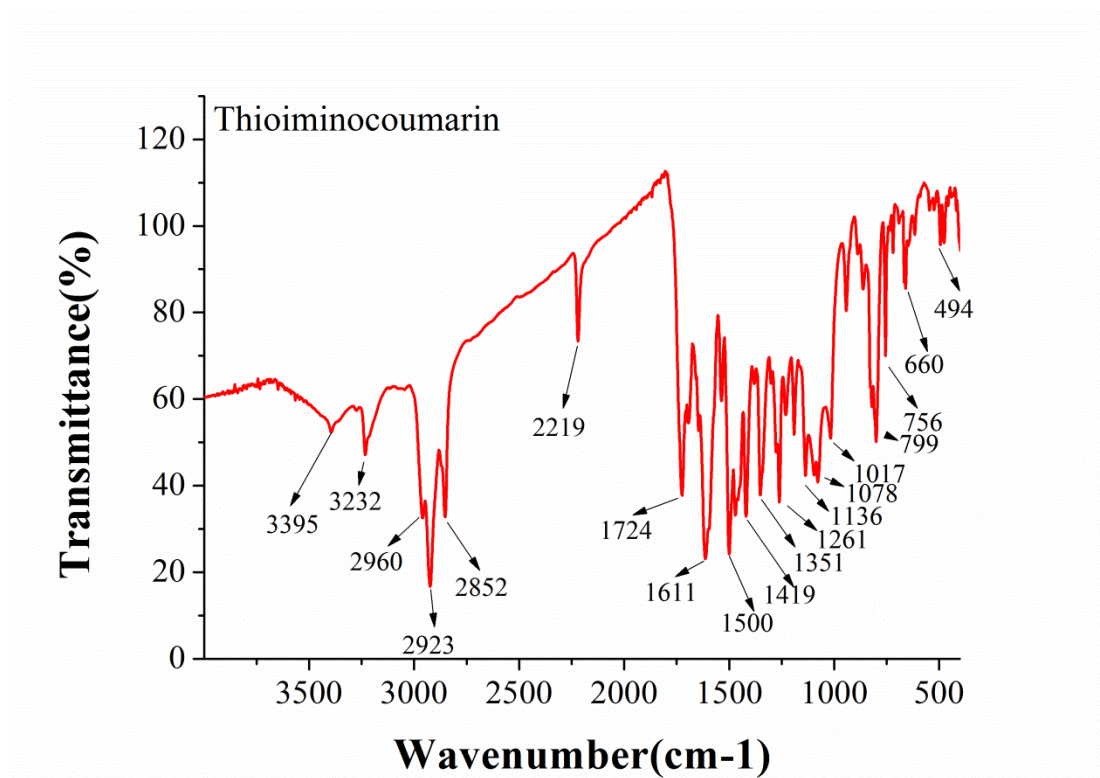


Fig. S61 FTIR spectrum of 7.

References

1. J. Liu, Y. Q. Sun, Y. Huo, H. Zhang, L. Wang, P. Zhang, D. Song, Y. Shi, W. Guo, J. Am. Chem. Soc., 2014, 136, 574.